KONYA FOOD AND AGRICULTURE UNIVERSITY

INSTITUTE OF NATURAL AND APPLIED SCIENCES

BIOTECHNOLOGY PROGRAM

FEEDBACK CONTROL OVER PHOTODYNAMIC ACTION

MASTER OF SCIENCE THESIS

Mediha Nur Zafer YURT

KONYA

DECEMBER, 2018

KONYA FOOD AND AGRICULTURE UNIVERSITY
INSTITUTE OF NATURAL AND APPLIED SCIENCES

FEEDBACK CONTROL OVER PHOTODYNAMIC ACTION

Mediha Nur Zafer YURT

Thesis Advisor: Assist. Prof. Sündüs ERBAŞ ÇAKMAK

Biotechnology Program

Meram-KONYA

DECEMBER, 2018

I certify that I have read this thesis and that in my opinion it is fully adequate, in scope and in quality, as a thesis of the degree of Master

....

Assist. Prof. Sündüs ERBAŞ ÇAKMAK (Advisor)

I certify that I have read this thesis and that in my opinion it is fully adequate, in scope and in quality, as a thesis of the degree of Master

....

Assoc. Prof. Mahmut Deniz YILMAZ

I certify that I have read this thesis and that in my opinion it is fully adequate, in scope and in quality, as a thesis of the degree of Master

....

Assoc. Prof. Fazlı SÖZMEN

I certify that I have read this thesis and that in my opinion it is fully adequate, in scope and in quality, as a thesis of the degree of Master

....

Prof. Menşure ÖZGÜVEN

Director of the Institute of Graduate School of Biotechnology

Mediha Nur Zafer YURT tarafından yüksek lisans tezi olarak sunulan "Fotodinamik Akvitenin Geri Besleme Döngüsüyle Kontrolü" başlıklı bu çalışma KGTÜ Lisansüstü Eğitim ve Öğretim Yönetmeliği ile KGTÜ Fen Bilimleri Enstitüsü Eğitim ve Öğretim Yönergesi'nin ilgili hükümleri uyarınca tarafımızdan değerlendirilerek savunmaya değer bulunmuş ve ../../2018 tarihinde yapılan tez savunma sınavında aday oybirliği/oyçokluğu ile başarılı bulunmuştur.

Jüri Üyeleri: **İmza:**

Jüri Başkanı   : Sndış Erbaş Çakmak   ....

Raportör Üye   : M.Deniz Yılmaz   ....

Üye   : Fazlı SÖZMEN   ....

This study titled "Feedback Control over Photodynamic Action" and presented as Master Thesis by Mediha Nur Zafer YURT has been evaluated in compliance with the relevant provisions of KFAU Graduate Education and Training Regulation and KFAU Institute of Science Education and Training Direction and jury members written below have decided for the defense of this thesis and it has been declared by consensus/majority of votes that the candidate has succeeded in thesis defense examination dated.

Jury Members: **Signature:**

Head   : Sndış Erbaş Çakmak   ....

Rappoeteur Member   : M.Deniz Yılmaz   ....

Member   : Fazlı SÖZMEN   ....

ÖZET

FOTODİNAMİK AKTİVİTENİN GERİ BESLEME DÖNGÜSÜYLE KONTROLÜ

YURT, Mediha Nur Zafer

Yüksek Lisans Tezi, Biyoteknoloji Anabilim Dalı

Tez Danışmanı: Dr. Öğr. Üyesi Sündüs ERBAŞ ÇAKMAK

Aralık, 2018, 72 sayfa

Kendine etkiyerek kendi aktivitesini kontrol edebilen etkileşim ağları biyoloji, ekonomi ve mühendislik dahil olmak üzere çok çeşitli alanlarda kompleks sistemlerin yüksek düzeyde kontrolünü sağlar. Patern oluşumu, kol-bacak gelişimi ve sirkadiyen ritim gibi biyolojik süreçler gen ifadesinden ekosistem seviyesine her aşamada dengeyi korumak için geri besleme döngüleriyle kontrol edilir. Fotodinamik terapi (FDT) temel olarak yüzey kanserlerini ve kimi cilt hastalıklarını tedavi etmek için kullanılır. Literatürde belirli koşullarda aktifleşen fotosensitizörler (FS) çalışılmasına rağmen, geri besleme döngüsüyle aktivitesi kontrol edilebilen fotodinamik terapi ajanları henüz araştırılmamıştır. Bu çalışmada, fotodinamik ajanının kendi aktivitesinin FS, $^1O_2$, askorbat ve peroksidin oluşturduğu negatif geri besleme döngüsüyle azaldığı gösterilmiştir. Üretilen $^1O_2$ askorbat varlığında perokside dönüşmekte ve FS yapısındaki boronatı oksitleyerek fotodinamik ajanını inaktif hale getirmektedir. PDT ajanının mitokondride biriktiği, ışıkla hedef hücreleri öldürdüğü ve inaktif olan geri besleme ürününün hücredeki etkisinin azaldığı gösterilmiştir. Kendiliğinden inhibe olan kontrol mekanizmasıyla yeteri kadar sitotoksik $^1O_2$ ürettikten sonra inaktif hale gelebilecek FDT ajanı, FDT'nin yan etkilerini azaltma potansiyeline sahiptir.

Anahtar sözcükler: geri beslemeli kontrol, fotodinamik terapi

ABSTRACT

FEEDBACK CONTROL OVER PHOTODYNAMIC ACTION

YURT, Mediha Nur Zafer

MSc in Biotechnology Program

Supervisor: Assist. Prof. Sündüs ERBAŞ ÇAKMAK

December, 2018, 72 pages

Auto-acting networks of interactions provide higher level control over many complex systems of diverse disciplines including biology, economy and engineering. Biological processes including pattern formation, limb development and circadian clocks are controlled by interaction between pathway elements via feedback loops maintaining homeostasis at every level from gene expression to ecology. Photodynamic terapy (PDT) is mainly used to treat surface cancers and certain skin diseases. Although certain activation modes for photosensitizers (PS) are reported in literature, no feedback regulated PDT activity is explored yet. Here, photodynamic activity of a PS is shown to be reduced through a negative feedback loop generated by PS, singlet oxygen, ascorbate and peroxide. Reaction of $^1O_2$ with ascorbate generates peroxide which oxidises boronate moiety of the PS, converting it into inactive form. PS is shown to accumulate in mitochondria and cell viability is shown to decrease significantly upon irradiation whereas feedback loop product is shown to have reduced effect on cell viability. Self-inhibitory control mechanism may make PDT more non-invasive since PS can be adjusted to shut down itself once certain amount of cytotoxic $^1O_2$ is produced.

Keywords: feedback control, photodynamic therapy

ACKNOWLEDGEMENTS

Dedicated to my advisor for all guidence in research and life

YEMİN METNİ

Yüksek lisans tezi olarak sunduğum "Fotodinamik Aktivitenin Geri Besleme Döngüsüyle Konrolü" adlı çalışmanın tarafımdan bilimsel ahlak ve geleneklere aykırı düşecek bir yardıma başvurmaksızın yazıldığını ve yararlandığım eserlerin bibliyografyada gösterilenlerden oluştuğunu, bunlara atıf yapılarak yararlanılmış olduğunu belirtir ve bunu onurumla doğrularım.

28./12/2018

Mediha Nur Zafer YURT

TEXT OF OATH

I declared and honestly confirm that my study titled "Feedback Control over Photodynamic Action" and presented as Master's Thesis has been written without applying to any assistance inconsistent with scientific ethics and traditions and all sources I have benefited from are listed in bibliography and I have benefited from these sources by means of making references.

28..12/2018

Mediha Nur Zafer YURT

TABLE OF CONTENTS

LIST OF FIGURES

TABLE OF CONTENTS

LIST OF ABBREVATIONS

AA: Ascorbic Acid

BODIPY: 4,4-difluoro-4-bora-3a,4a-diaza-s-indacene

CRC: Colorectal Cancer

DMSO: DimethylsulfoxideDNA:

DPBF: Diphenylbenzofurane

EET: Electronic Energy Transfer

EPR: Enhanced Permeation and Retention

FRET: Förster - Type Energy Transfer

HOMO: Highest Occupied Molecular Orbital

HPA: Hypothalamic – Pituitary – Adrenal axis

HRMS: High resolution ESI-MS

IC: Internal Conversion

IC_{50}: Half Maximal Inhibitory Concentration

ICT: Intramolecular Charge Transfer

IR: Infrared

ISC: Intersytem Crossing

LED: Light Emitting Diod

LUMO: Lowest Unoccupied Molecular Orbital

NIR: Near Infrared

NMR: Nuclear Magnetic Resonance Spectroscopy

PBS: Phosphate Buffered Saline

PDT: Photodynamic Therapy

PeT: Photo - induced Electron Transfer

PS: Photosensitizer

RET: Resonance Energy Transfer

RNA: Ribonucleic Acid

ROS: Reactive Oxygen Species

RPMI: Roswell Park Memorial Institute

SA: Sodium salt of ascorbate

TBHP: Tert Butyl Hydroperoxide

TLC: Thin Layer Chromatography

CHAPTER 1

INTRODUCTION

Photodynamic therapy (PDT) is based on photoactivation of certain chemicals termed photosensitizer (PS) to generate cytotoxic singlet oxygen and initiate selective cell destruction in desired area. From the discovery, PDT has been used for treatment of certain cancer types such as head and neck region, lung, gastric, servical cancers as well as non – oncological diseases like microbial, viral and skin related disorders like acne (Robertson et al, 2009; Zhang et al, 2018). Although the treatment is known for over 100 years, PDT has been broadly accepted and utilized only for many years in clinical applications. From the point of selectivity, non – invasiveness, fast result, lower costs and wide therapeutic window, PDT has become promising treatment modality for both malignant and non – malignant diseases. One of success of the treatment based on the locatization and activation of photodynamic agent. In literature, activation of photosensitizer with certain modes are widely studied however control of photodynamic action through feedback loops is not investigated. This thesis introduces a novel photodynamic agent that control its activity by feedback mechanism. Feedback control are a general control mechanism enabling communication between output of a system with the system itself, and used to control many different complex processes (Cinquin and Demongeot, 2002). Control mechanism over action simply consist of following steps; generation of singlet oxygen, transformation of singlet oxygen into hydrogen peroxide. Produced hydrogen peroxide oxidizes boronate moiety of PS upon which, PS turn into inactive form. Designed photosensitizer enables intersystem crossing by charge transfer character generated through pyridinium moiety, however boronate deprotection convert the molecule into a derivative having less charge transfer character. Hence, PS becomes

inactive. Moreover, positively charged PS show tendency to accumulate in mitochondria due to boronate moiety is attached to the BODIPY core through pyridinium, creating a positive charge. Due to large membrane potential of mitochondira, lipophilic compounds can pass simply through lipid bilayers and accumulation induces by the potential gradient (Murphy, 2008). Thus, proposed PS offers photodynamic action in the certain organelle of the cell with an unexplored control mechanism. Altogether, this research suggests a novel approach for auto-controlled photodynamic activity.

CHAPTER 2

BACKGROUND INFORMATION

2.1. Basic Photophysics of a Fluorophore

Photophysics is associated with process of light when it interacts with atoms and molecules. Light – matter interaction results in two possible pathways: one of those pathways is scattering of light. The second possible pathway is absorption of light and subsequent emission at ultraviolet, visible or infrared photons from an electronically excited species. This type of emission is called luminescence and this chapter laid emphasis on basic principles of photoluminescence or competing deactivation pathways. Absorption of light, fluorescence and phosphorescence are particularly important in understanding photophysics of a compound together with alternative deactivation modes such as intersystem crossing (ISC), internal conversion (IC), vibrational relaxation (Valeur, 2012).

The interaction of light with molecules leads to photophysical changes. It refers to electronic transition, which means excitation of the compounds with light spark off transition of an electron from the ground state to an unoccupied orbital of higher energy called excited state. Electronic transition within the organic compounds containing heteroatom obey two major selection rules: spin – forbidden and symmetry – forbidden transition. In Figure 2.1 formaldehyde is used as an example of heteroatom containing organic molecule to display relative energy levels of molecular orbitals and electronic transition between them. According to molecular orbital theory two types of orbitals, sigma σ and pi π, have leading roles in molecular interactions of organic compounds. The $\pi \rightarrow \pi^*$ type transitions necessitate less energy when compared to $\sigma \rightarrow \sigma^*$

transition. Moreover, molecules also have non – bonding electrons located on heteroatoms like oxygen and nitrogen, denoted as n orbitals. Likewise transition of an electron to higher energy level by absorption of a photon can pass to an antibonding orbital from n orbitals. These transitions are symbolized as n → σ*, n → π*. Based on required energy, electronic transition generally follow the order: n → π* < π → π* < n → σ* < σ → π * < σ → σ*. Changing the substituents of an organic molecule can alter the relative energy levels as well as probability of electronic transitions. Two orbital types matter for absorption and fluorescence spectroscopy: Highest Occupied Molecular
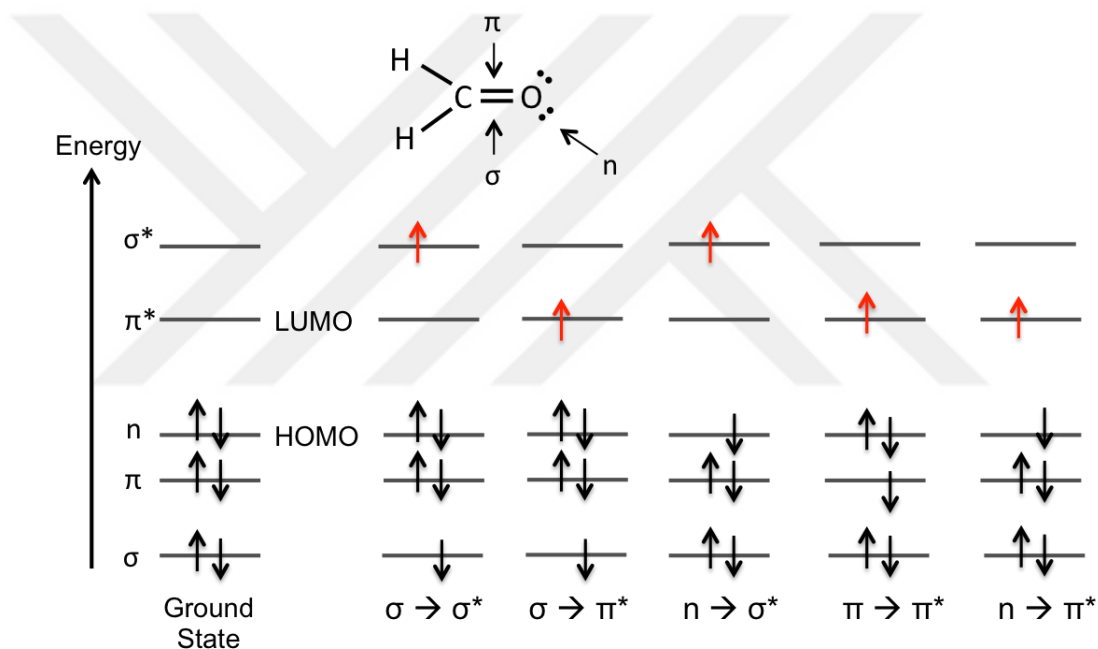
Figure 2.1. Relative energy levels of molecular orbitals in formaldehyde and possible electronic transitions.

Orbital (HOMO) and Lowest Unoccupied Molecular Orbital (LUMO). Both of these molecular orbitals point out ground state of molecule. An electron transition from HOMO to LUMO, like n → π* in heteroatoms, generally lead to redistribution of electron density on the molecule. This redistribution of electron density within the molecule may also refered as charge transfer. As compared with the ground state an increase in the dipole

moment is observed. Such charge transfer characters in heteroatom containing molecules are used in many applications including molecular sensors.

Spin quantum number of a molecule having two electrons of opposite spins in ground state is equal to zero (S=0) hence multiplicity of 1 (2S+1 = 1). Because of the multiplicities it's called singlet state as shown in Figure 2.2. In case promoted electron changes its spin, which means two electron of molecule located parallel spins at different molecular orbital, the spin quantum number equals to 1 and multiplicity is 3. It's called as triplet state as shown in Figure 2.2. Transitions involving a change in spin multiplicity is forbidden unless species have mixing of states such as in the case of spin orbit coupling (Marian, 2011).
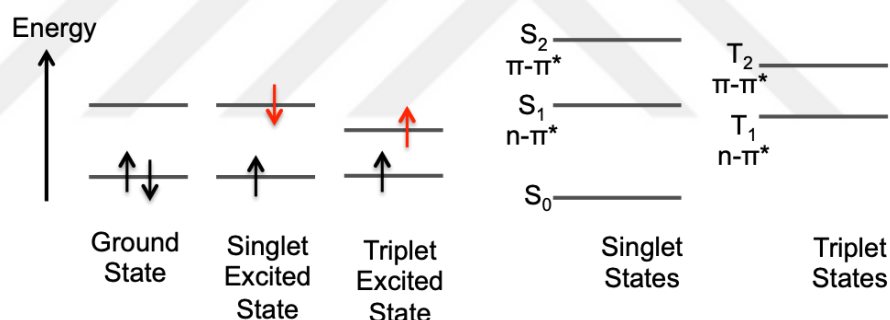
Figure 2.2. Singlet and triplet states of molecular orbitals using formaldehyde as an example.

Once the molecule is excited by a photon, emission can be through any of the following processes: fluorescence, phosphorescence or delayed fluorescence. Apart from them, there are also diverse physical pathways for deactivation such as internal conversion (IC), intersystem crossing (ISC), intramolecular charge transfer (ICT) and photoinduced electron transfer (PeT). Moreover, there are other pathways that compete with deexcitation through interaction of the excited state with other molecules through any of the processes: electron transfer, proton transfer, energy transfer and excimer or

exciplex formation. All of the mentioned possible pathways are illustrated in Jablonski Diagram named after Polish scientist Aleksander Jablonski (first proposed by Aleksander Jablonski, 1935). This diagram is shown in Figure 2.3. In the first column of diagram, blue arrows denoted as absorption is the essential process of excitation. Excitation takes place to higher vibrational energy levels of excited electronic states, and occurs tremendously fast (10^{-15} s) when compared to all other process hence during this process displacement of the nuclei is negligible. The purple arrows from the vibrational level of excited electronic state to vibrational ground state is called vibrational relaxation and show lower energy emission output. This difference between absorption and emission wavelengths due to vibrational relaxation after absorption is called Stoke's shift named after Irish phsicist George Gabrial Stokes (Stokes, 1852). The lifetime of the vibrational relaxation is relatively slower than absorption (almost 10^{-12} – 10^{-10} s).
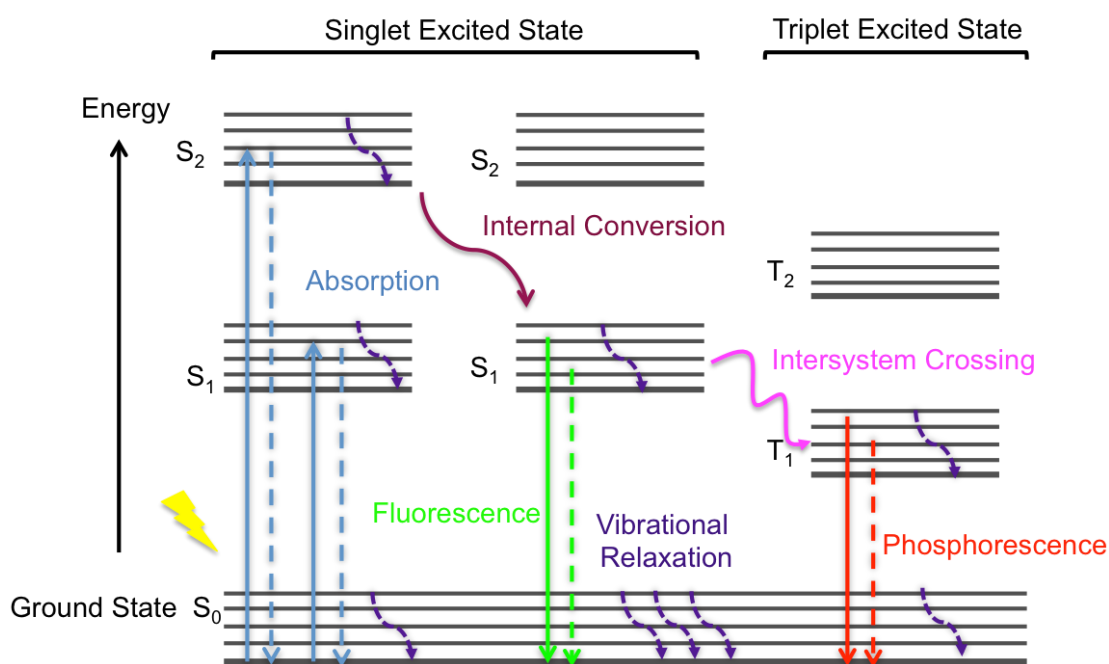
Figure 2.3. Jablonski Diagram, illustration of the possible photophysical processes following the excitation by photon.

One of the non – radiative transitions called internal conversion is shown with a maroon arrow and refers to transition between two electronic states of the same spin. In the case of vibrational relaxation, excess energy is transferred to the solution. The lifetime of the singlet state for most compounds is around $10^{-11} – 10^{-9}$ s. Amongst the possible deactivation processes, intersystem crossing follows a different pathway from other non – radiative transitions. Transition takes places in the following way; an excited electron from the level of S_1 moves to the level of triplet T_n and terminates at lowest vibrational level of T_1. Normally electronic transition between these two electronic states have different multiplicities, hence it is forbidden. However, creating a magnetic moment, for instance by the presence of heavy atom in a molecule allows spin – orbit coupling and mixed spin states makes the transition possible. The intersystem crossing system provides great application in the area of photodynamic therapy. Singlet oxygen ($^1O_2$), which is one of the major component of photodynamic therapy, produced from triplet state of the photosensitizer by energy transfer to molecular oxygen (Dougherty et al., 1998). Moreover, considering the lifetime fastness ($10^{-10} – 10^{-8}$ s), intersystem crossing can easily compete with other deactivation pathways.

Fluorescence (or emission) occurs during $S_1 \rightarrow S_0$ relaxation of an excited electron (Figure 2.3, green line). However, fluorescence takes places at higher wavelength with lower energy. Energy loss in the excited state can be explained by vibrational relaxation namely Stoke's shift. Fluorescence response is not as fast as absorption and there is exist a competition between this process and other deactivating pathways like internal conversion or intersystem crossing. For most fluorophores, lifetime of singlet excited state lasts for $10^{-10} – 10^{-7}$ s and shows characteristic exponential decay.

The last major type of photoluminescence is phosphorescence (Figure 2.3, red line). When we compared the other deexcitation pathways, phosphorescence lifetimes are longer, about $10^{-6} – 1$ s. In this type of deexcitation, $T_1 \rightarrow S_0$ transition observed with lower energy and higher wavelength than the fluorescence. Normally, such transition is forbidden but due to spin – orbit coupling, it can also occur at room temperature.

In addition to fate of excited electron mentioned above, energy transfer may be an alternative non – radiative deexcitation pathways among the molecules. This type of transition necessitates interaction between donor and acceptor molecules. It can only happen when the emission spectrum of donor overlaps with the absorption spectrum of acceptor (so called spectral overlap). Therefore, most of vibronic transitions in donor match with transitions in acceptor. Such coupled transitions between molecules named resonance and mostly verbalise resonance energy transfer (RET). There are two well – known types; Förster type resonance energy or electronic energy transfer (EET, FRET) and Dexter type energy or electron transfer. Förster type energy or electron transfer basically based on dipole interaction and donor-acceptor molecules should be close enough for interactions whereas Dexter type energy transfer requires direct electronic communication between species (Förster, 1946; Dexter 1973). FRET between rationally designed systems can provide wide range of applications, for instance in the analysis of ligand or stimulus induced conformational changes (Figure 2.4) (Lau et al, 2011). Conformational changes in biological system (i.e. proteins) may lead to separation of donor-acceptor leading to decrease in FRET or may bring the energy transfer modules closer thus enhance the fluorescence of the acceptor.
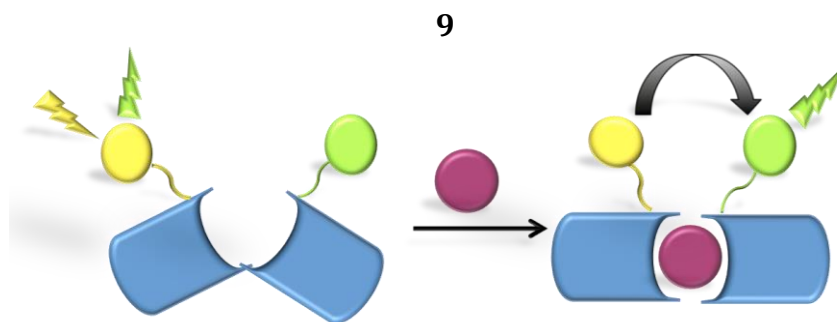
Figure 2.4. Schematic representation of ligand induced conformational changes. Ligand binding leads to conformational changes, that brings the energy transfer modules (donor and acceptor fluorophores) closer, FRET efficiency increases as a result.

Photoinduced electron transfer, another possible deactivation pathway, occurs in the following way; transition of an electron from HOMO of the auxillary moiety (such as ligand part) to the HOMO of the fluorophore takes place hence this transition completes with fluorescence of the fluorophore (since HOMO of the fluorophore is occupied by this reduction, excited electron can not turn back to ground state shown in Figure 2.6), as shown in Figure 2.5 (de Silva et al, 1997).
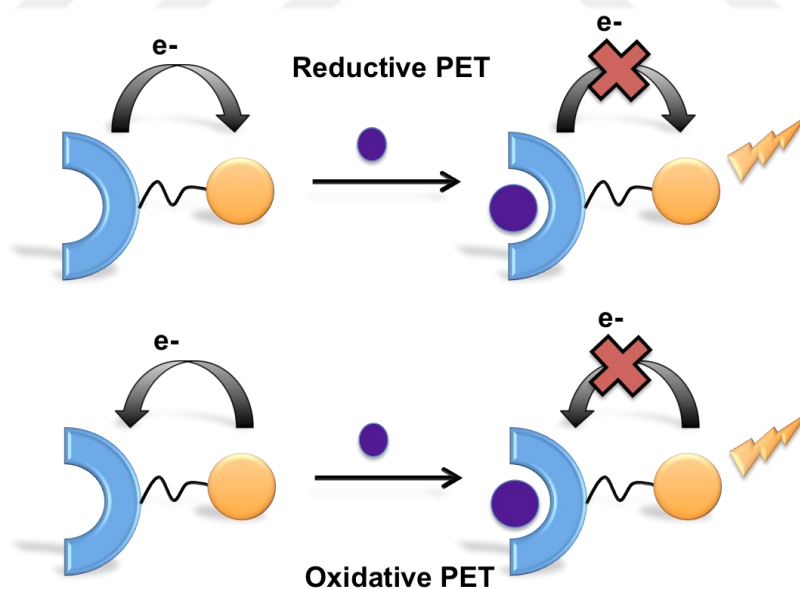
Figure 2.5. PeT Types and possible sensor application. Reductive PeT occurs when electron transfer takes place from HOMO of the auxillary module to the HOMO of the fluorophore. Oxidative PeT results in reduction of auxialary moiety through electron transfer from LUMO of the excited fluorophore. In either case analyte binding may change HOMO and/or LUMO levels enabling change in PeT efficiency.

Apart from this reductive PeT, an alternative oxidative PeT can take place when LUMO of the ligand energitically lies close to LUMO of the fluorophore. In this case, electron transition takes places between the LUMO of the excited fluorophore to the lower LUMO level of ligand. PeT mechanism can provide control over fluorescence outcome if properly designed fluorophore and ligand assemblies exist. It is widely used in molecular chemosensor applications (Mclaughlin, 2018).
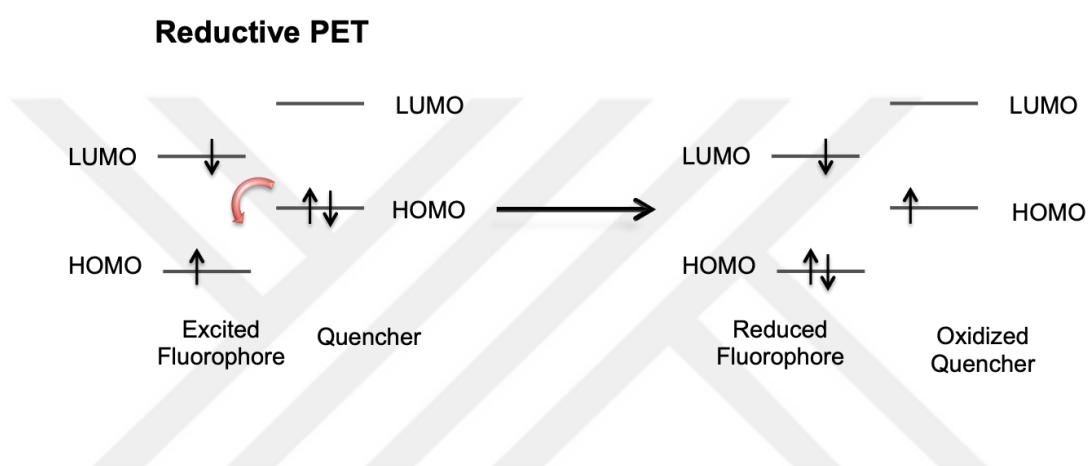
Reductive PET

Figure 2.6. Mechanism of reductive PeT. Excited fluorophore is reduced through electron transfer from neighboring group.
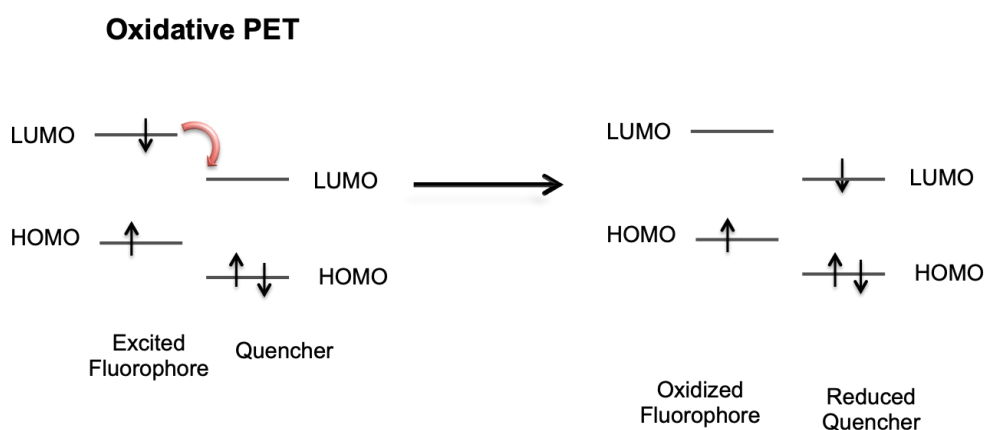
Oxidative PET

Figure 2.7. Mechanism of oxidative PeT. Excited fluorophore is oxidized through electron transfer to the neighboring group.

After excitation of a fluorophore, electron is transferred from one orbital to another. Since electron distribution within the molecule differs between initial and final orbitals, dipole moment of fluorophore may change dramatically. In the presence of electron donating and electron withdrawing groups in conjugated molecules, dipole moment usually increases distinguishably. Upon excitation of fluorophore, the redistribution of charge over the molecule continues until thermodynamic equilibrium between solvent and fluorophore is reached. In the end of excitation, solvent molecules rotate and affect fluorescent properties. After relaxation, molecules attain intramolecular charge transfer (ICT) state. By the changing of solvent, ligand binding and polarity properties, fluorescent characteristics can change and this photoinduced ICT can be used to design ideal analyte - receptor interaction. Therefore, it can find application in analyte or environment sensing platform.

2.2. Photodynamic Therapy

Light has been used in the therapy of many diseases for thousands of years and this therapeutic method dates to Ancient Egyptian civilization. However, combination of light and photosensitive chemicals recorded first with accidental observation of Paramecia microorganism in 1890s (Raab, 1900). Then, Prime's (1900) studies about treatment of dermatitis by using eosin dye was reported as the first clinical application of light. Another pioneering application with the use of light was in 1900s. Tappeiner et al, suggested a new method for the treatment of skin tumors with the use of topical eosin and light (von Tappeiner and Jodbauer, 1903). Later, based on the researches on this field, oxygen reported as crucial component of this mechanism and "photodynamic action" is

started to be used to define the behavior of the photosensitizer-light and oxygen combinatorial reaction (Tappeiner, 1904). Since from discovery, photodynamic therapy (PDT) becomes a promising clinical application for certain cancers, microbial, viral or non - malignant diseases like infection.

Photodynamic therapy consists of three essential elements, these are a photosensitizer (PS), oxygen and light source. PDT action is based on excitation of photosensitizer with specific wavelength of light and transferring the energy from the excited photosensitizer to the molecular oxygen in order to induce cell death. Cell death occurs through cytotoxic singlet oxygen ($^1O_2$) generated from molecular oxygen. Since in order to have photodynamic action, photosensitizer is needed to be activated by light, and light is introduced to a particular region of the cell (i.e. disease site), PDT shows non-invasive character. Induced cell death by irreversible oxidative damage of biomolecules happens within a short time (6 ns) and diffusion distance of singlet oxygen (< 2 nm) makes PDT as non – invasive treatment (Skovsen et al 2005; Josefsen and Boyle, 2008).

Ground state of molecular oxygen is found in a triplet state, a non - reactive form. During photodynamic action, excitation of photosensitizer follows sequential reactions. First a transition from singlet excited state to triplet state takes place through intersystem crossing (ISC) and energy transfer from the triplet state to molecular oxygen generates singlet oxygen in media. Produced highly toxic singlet oxygen reacts with organic compounds including lipids, amino acid residues and also nucleic acids (RNA or DNA) very fast and gives oxidative damage to the cell (Skovsen et al 2005). When PDT is applied with sufficient dose of photosensitizer for enough time, only irradiated cells in target location like cancer cells, go through apoptosis or necrosis as a result of oxidative damage mentioned above.

2.2.1. Physical and Biochemical Mechanism of Photodynamic Action

Singlet oxygen generation yields by photodynamic action is determined by intersystem crossing efficiency compared to other deactiactivation pathways. In this case transition to triplet excited state via singlet excited state ocurs. Aforementioned forbidden transition between two electronic states having different multiplicities enhanced by presence of heavy atom, certain orthagonal structures or mixed spin states. Moreover, certain molecules with charge transfer character are shown to have efficient ISC (Harriman et al, 2007; Awuah and You, 2012). During photodynamic therapy singlet oxygen is not the only intermediate molecule generated, the other reactive oxygen species and radicals are also produced. After excitation of a photosensiztizer, excited triplet state can follow two possible pathways, as shown in Figure 2.8. During the first of these pathways, excited ptohosensitizer can react with a substrate (cell components) directly to produce radical species. As a result of type I reaction, produced radicals interact instantaneously with molecular oxygen to generate mixture of reactive oxygen intermediates such as superoxide and hydroxyl radicals or other reactive peroxides such as hydrogen peroxide.
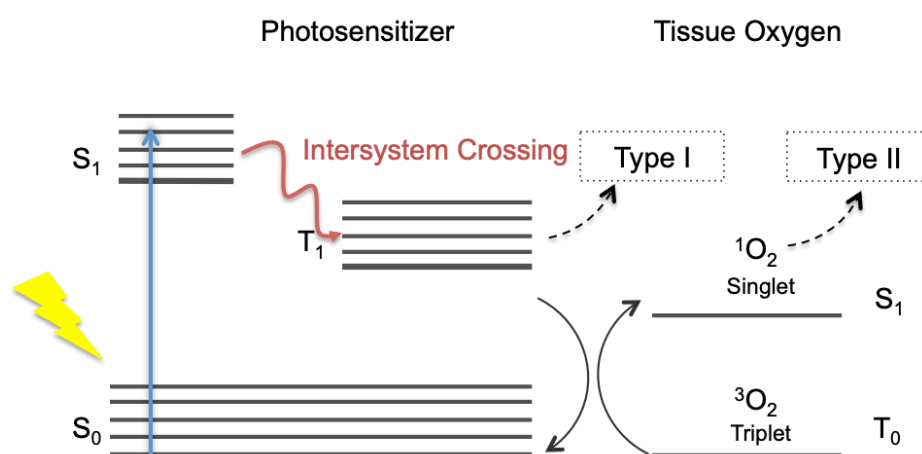
Figure 2.8. Partial Jablonski Diagram and type I and type II reactions involved in PDT action. Type I reactions involves direct damage given to biomolecules from the photosensitizer. Type II reaction involves generation of singlet oxygen intermediate.

In the second pathway named type II reaction, triplet states of photosensitizer transfer its energy to ground state molecular oxygen to generate singlet oxygen. Particularly, type II reaction of photodynamic action have major contribution to photo – induced cell death mediated by cytotoxic singlet oxygen. However, both type of reactions take place simultaneously. Type of photosensitizer effects the ratio of the reactive oxygen products. Also substrate concentration, binding affinity of sensitizer and local enviroment determines the type of reaction involved in PDT action (Gomer and Razum, 1984). Moreover, due to short half – life of produced oxygen intermediates and high reactive nature, PDT action is highly localized, providing a way of passive targetting.

Sufficient and fixed energy from light provide a source of energy to stimulate photosensitizer. Photosensitizer transfers energy to reactive oxygen species and produced ROS give oxidative damage to target cell, basically gives damage to cell membrane and interferes with protein folding and result in production of non – functional proteins (Davies and Truscott, 2001). As a result of disturbing cell structure, biological systems tend to go cell death. After application of photodynamic therapy, cells can directly go to apoptosis, necrosis or autophagy. An indirect effect of PDT is initiation of anti – tumor immune response (Gollnick and Brackett, 2010). PDT also cause damage to tumor vasculature by which supply to tumor tissue becomes restricted (Figure 2.9) (Chen et al, 2005). One of the results of oxidative damage in the cell mediated by singlet oxygen is lipid peroxidation. This leads to cell membrane leakage by disintegration of lipids and proteins. Moreover, these disrupted lipids elements stimulate immune responsive molecules and that cause cell death in multiple way (Wright, 2003; Dabrowski et al, 2016).
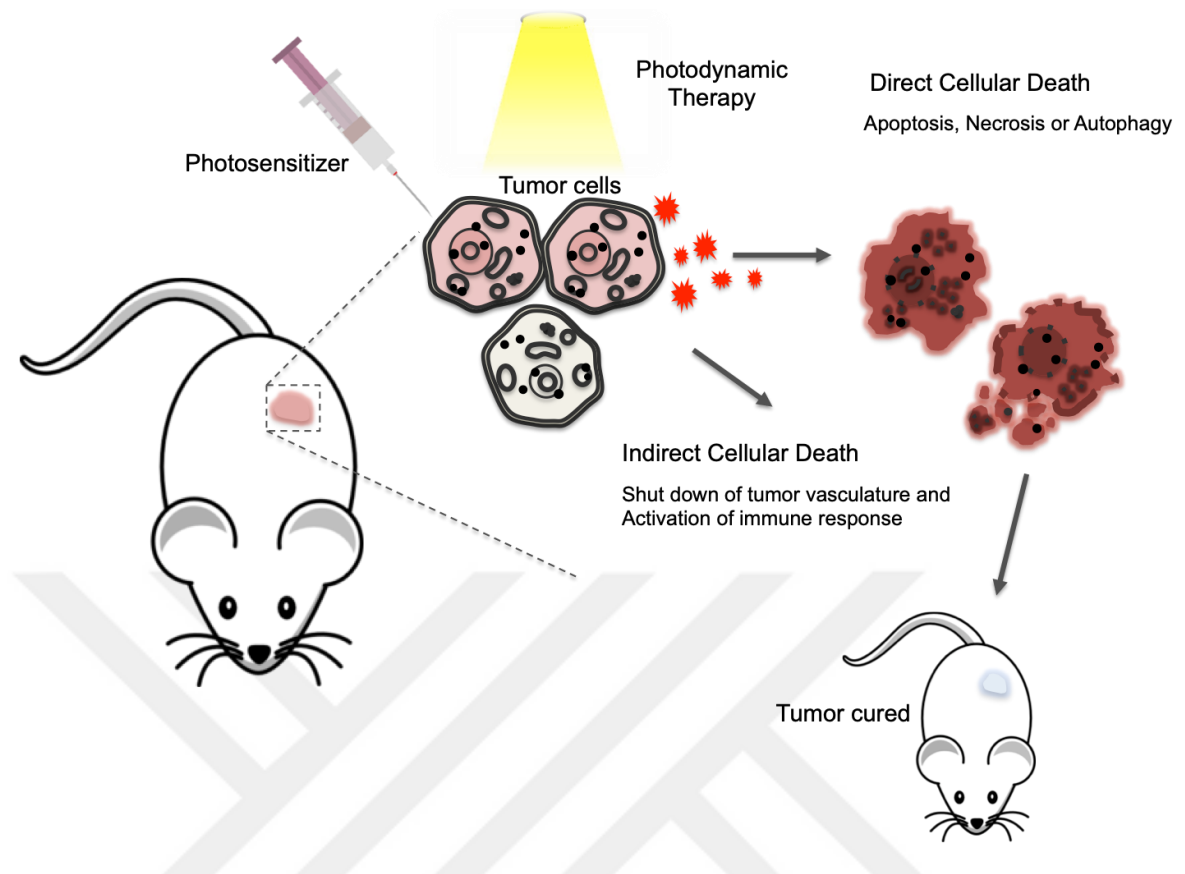
Figure 2.9. The application of PDT based on destruction of tumor cell presence of light and oxygen. Cellular death can be induced both directly (apoptosis, necrosis or autophagy) or indirectly (activation of anti – tumor response or shut down tumor vasculature).

Proteins and amino acids are essential elements of cells in the way of both cell functionality and membrane structure. Protein are affected from PDT action by oxidation of thiols and amines of amino acids cause production of non – functional proteins. Particularly that induce mitochondrial membrane leakage, inducing cell death. Moreover, genetic materials affected from produced reactive oxygen species. Genotoxic damage reveal in different ways such as DNA strands breaks, which may result in mutation. PDT induced damage on DNA takes place on thymine groups reaction with produced hydroxyl radicals. Interrupted genetic materials and accumulated mutations induce apoptosis (Cadet and Mascio, 2006).

Successful elimination of tumor tissue by photodynamic action is achieved in many different cancer types. This method is used clinically for treatment of wide range cancers including basal – cell carcinoma, cervical cancer, lung cancer, gastric cancer, head and neck cancer (Sharman et al, 1999). Moreover, PDT is used for other non – malignant diseases like age – related macular degeneration, rheumatoid arthritis, papilloma virus and skin related disorders like acne (Wang et al, 2000) . Regional light treatment provides minimally invasive and less toxic treatment strategy. However, efficacy of photodynamic action depends on light delivery to target location. For this reason, current effective applications mostly based on tumors on surfaces of the body such as on skin or non – internal organs. Moreover, performance of PDT also relies on efficiency of photosensitizer to produce singlet oxygen. Activation with long wavelength of light (with high tissue penetration) and elimination of dark toxicity are also required in PDT (Jang et al, 2006). Altogether, photodynamic therapy is promising method in the way of less side effects, non – invasiveness, fast response time, possibility of precise targeting, repeatability, lack of scarring and cost effectiveness.

2.2.2. Activatable Photodynamic Agents - BODIPY Photosensitizers

Since photodynamic action basically necessitate photosensitizer activation with light and transferring energy to oxygen, activity can be regulated by irradiation time. Like any other therapeutic agents, photosensitizer tend to accumulate in tumor tissue due to leaky membrane structure and increased vasculature of these tissue and this fact termed enhanced permeation and retention (EPR). This passive targetting provide accumulation of the photosensitizer in the tumor tissue, provide further selectivity necessary to protect nearby healthy cells. In order to improve nontoxicity to healthy cells, designed ptohosensitizers should piled up preferentially tumor cells. In order to achieve efficient

excitation in deep tissue, photosensitizer are expected to have high exctinction coefficients at long wavelength region of spectrum (IR or Near IR reagion) to enable the use of deep-tissue penetrating light.

Recently, BODIPY (4,4-difluoro-4-bora-3a,4a-diaza-s-indacene) photosensitizer has emerged with many characteristic asked from an ideal photosensitizer. BODIPY derivates widely used for fluorescence imaging due to high fluorescence quantum yields and high exctinction coefficients, easily functionalization by chemical modification, resistance to photobleaching, high cellular uptake and low dark toxicity. Certain modifications also make BODIPY compounds efficient photodynamic agents. To enable ISC, halogenation of BODIPY core (the heavy atom effect) can be done easily (Kamkaew et al, 2013). Substitution by amine bearing neighboring groups, photo – induced electron transfer can be achieved which may be used for various device application. Functionalization of the BODIPY core enables production of BODIPYs having different photophysical properties: such as those having different absorption and emission spectra, excited state dynamics or extinction coefficients (Lovell et al, 2010). Thus, BODIPY nominates promising clinic PDT agent for future applications.

2.3 Feedback Loops as A Way of Control Mechanism

Feedback is indispensable mechanism required to maintain life. The mechanism regulates every interaction and response at every level of organism from cell to ecosystem (Åström, 2008). Basically, feedback is based on cause and effect loop such that output changes the first or other previous steps of sequence of reactions. This back-acting enables a communication between systems output and the system itself. Thus, feedback

mechanism can be considered as a powerful tool to control the activity of many different systems when designed properly.

Intrinsic and extrinsic parameters can alter and influence the biological systems. In order to keep system under control within the optimal level and to resist against abrupt changes, biological systems develop complex control mechanisms. By using feedback characteristic, the system can regulate its activity to respond to new condition. As a result of feedback activity, systems can carry on the activity in such a way that system remains balanced, more sensitive and/or stable. Such dynamic feedback systems can adapt to even diffucult conditions (Wotherspoon and Hubler, 2009) .

As mentioned, biological parameters should be regulated within the narrow range in order to maintain life. For example, level of insulin changes in blood shows an oscillation to meet the needs of organism (Hellman, 2007). Therefore, based on the cause and effect interaction, there are many types of feedback control mechanism. Negative and positive feedback are common in biological systems. The term negative and positive do not point to good or bad results. A negative feedback loop slow down the operation by its intermediate or final product through inhibition of the previous steps, whereas potisitive feedback loop reinforce and accelerate the process by activating it further (Figure.2.10).

One of the intriguing example proves the importance of negative feedback mechanism. In normal tissue, cell growth and division stay under control regulated by adhesion properties of cell surfaces and regulation of intermediates of cell proliferation to preserve tissue integrity and inhibit uncontrolled division (Vlahopoulos et al, 2015).
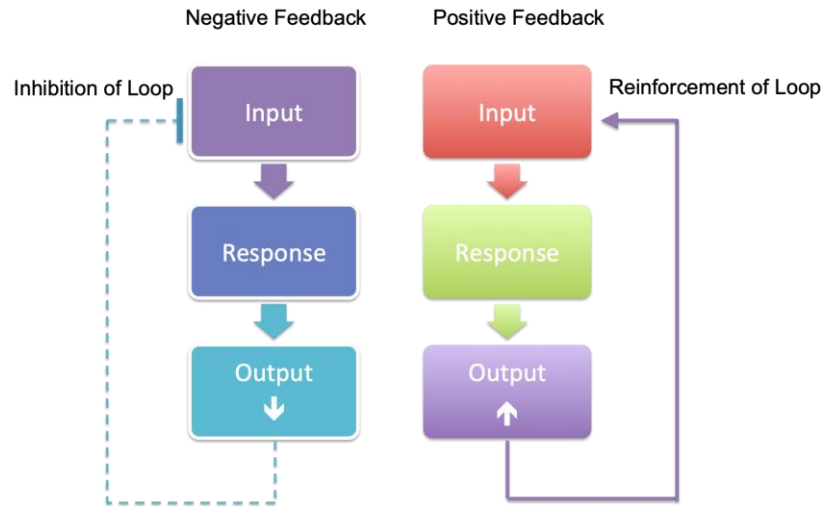
Figure 2.10. Types of Feedback Mechanism. Negative feedback loop inhibited by its own output whereas positive feedback loop's activity enhances through accumulation of output.

However, collapse in the feedback can disrupt the interaction between mediator molecules and unregulated cell growth and proliferation follows, causing development of tumor cells. On the other hand, inflammatory mediators secreted from injured cells like tumor tissue induce feedback response in immune system (Kornev et al, 2017). Stimulated immune system reinforce its own cell division by positive feedback to restore injured tissue structure and function.

Not only physiological functions but also regulation of gene expression is maintained by feedback control. Operons activities of genes are controlled by various repressor and activator proteins. In 1961, Francois Jacob and Jacques Monod introduced the feedback mechanism is protein synthesis and its genetic control in bacteria. Lac operon mechanism based on regulataion of sugar molecules in bacterial cells. The mechanism can go both way positively accelerate or negatively slow down based on stimulator concentration. On a larger scale, ecocsystem is also controlled by feedback mechanism. Population of community regulated by negative feedback based on prey –

predator relation (Holling, 1973). Most of hormones controlled by positive feedback mechanism. As an example, hypothalamic – pituitary – adrenal axis (HPA axis) consist of three elements and their feedback interaction regulates stress response (Nestler, 2015).

In the project presented in this thesis, a negative feedback loop is used to control activity of a photosensitizer. Although afore mentioned importance of feedback control mechanisms are well known, up to date there are no bioactive compounds reported having such complex regulation property. Hence, the mechanism introduced in this thesis may provide a new inside in the drug design.

CHAPTER 3

DESIGN OF THE PHOTODYNAMIC THERAPY AGENT

Several photosensitizers with different activity control mechanism have been studied recently, most of them have the ability to be activated with one or more stimulus such as presence of certain enzymes, low pH or glutathione (Lovell et al, 2010, 2011; Tian et al 2015; Zhao et al, 2015). However, post-action activity control has not been explored yet. The concept of feedback provide control of activation by desinging negative feedback loop which inhibits through its own product. This novel afford the keep activation of photosensitizer under control like most of biological system.

In order to decrease the cytotoxicity of the photosensitizer after potential treatment procedure, a feedback-controlled agent is proposed. With these goals, designed a photosensitizer BOD 2 shown in Figure 3.1, which can dissolve in and be activated both in water and organic solvents, generate cytotoxic singlet oxygen when irradiated with 506 nm LED array. Molecule has the ability to respond to hydrogen peroxide selectively and this property is used to incorporate feedback control over activity.
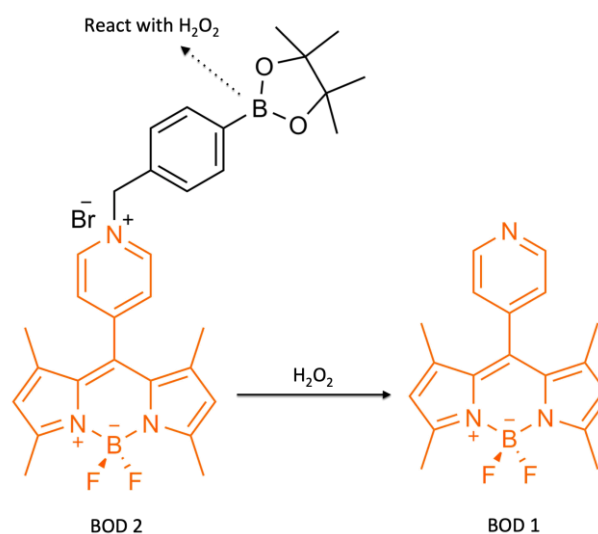

Figure 3.1. BOD 2 gives reaction with H_2O_2 through boronate moiety. As a result of reaction highly fluorescent BOD 1 forms.

The target compound BOD 2 consists of two major parts, which are BODIPY core and boronic pinacol ester attached to the core via pyridinium moiety. Previous studies showed that BODIPY (4,4-difluoro-4-bora-3a,4a-diaza-s-indacene) dyes are well – known fluorophores serve noticeable purposes such as targeting specific region of the cell and allow wide range of functionalization. Fluorescence and or PDT action of derivatives of such compounds are reported to be controlled by photo-induced electron transfer (PeT) or Förster resonance energy transfer (FRET) (Loudet and Burgess, 2007).

Designed compound BOD 2 generate cytotoxic singlet oxygen when excited at fixed wavelenght thorough promoting intersytem crossing (ISC). Even though ISC requires assistance of heavy atoms (such as I, Br), certain orthagonal structures and pyridinium BODIPY derivatives are extensively studied and shown to have efficient ISC (Harriman et al, 2007). Pyridinium BODIPY derivatives are used as molecular sensors but the photodynamics activities are not investigated yet.

Ever since the boronate esters are used in the design of peroxide sensors in 2004 by Chang and coworkers, detection of hydrogen peroxide at cellular level with the use of same motif has afforded with high recognition and reactivity (Miller et al, 2005, 2007; Albers et al, 2006; Dickson and Chang, 2008; Lippert et al, 2011). This approach depend on ambiphilic reactivity of hydrogen peroxide. Most of reactive oxygen speices shows similar shape, size and transient nature. Different from those hydrogen peroxide can behave as both nucleophile and electrophile. Due to O – O bond structure, hydrogen peroxide react as two electron electrophilic oxidant and non – bonding orbitals of oxygen atom allows to behave as efficient nucleophile. This ambiphilic structure perfectly harmonize with boronates upon reacting with electrophilic moiety at first, then become capable of reacting with nucleophilic moiety. Therefore, designed compound BOD 2 with

boronate ester in the structure, shows high selectivity hydrogen peroxide over other reactive oxygen species (Lippert et al, 2011).

The target compound BOD 2 incorporated with alkylated pyridinium which promote photo – induced electron transfer (PeT) via electron transfer to low lying LUMO of pyridinium and has efficient ISC required for photodynamics action (Harriman et al, 2007). Although ISC of similar pyridinium structures are calculated no photodynamic activity mesurement is done with heavy-atom free pyridinium BODIPY derivatives. When boronate moiety react with hydrogen peroxide, the boronic ester converted to an electron donating phenol followed by spontaneous 1,4 – elimination reaction (Xu et al, 2014; Lampard et all, 2018) and as a result of this reaction pyridinium is converted into pyridine and photo – induced electron transfer is interrupted. Hence generated BODIPY (BOD1) has strong fluorescence signal. Reaction of BOD2 with H_2O_2 to generate BOD1 is shown in Figure 3.2.

In order to control the activity of BOD 2 by a feedback system, conversion of singlet oxygen to hydrogen peroxide is used. Since hydrogen peroxide destroy pyridinium structure which is necessary for photodynamic action, a feedback control system which
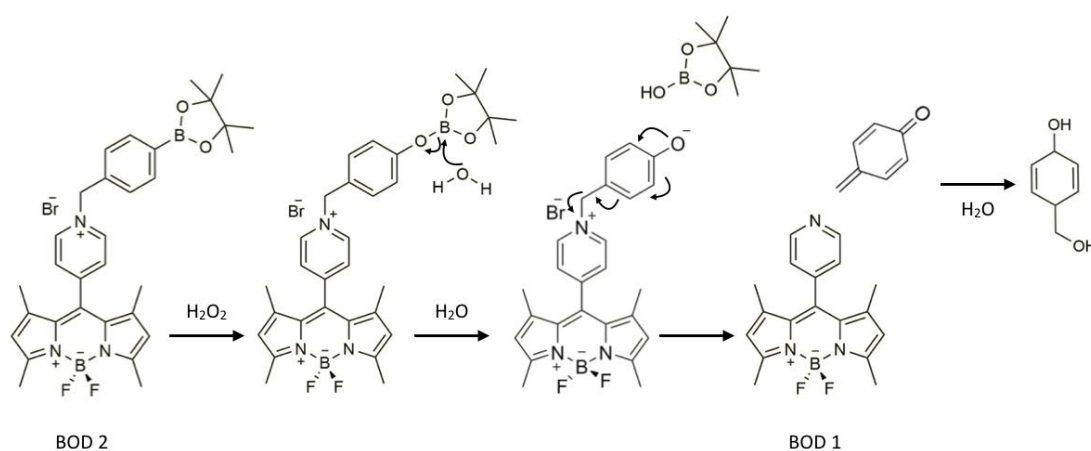
Figure 3.2. Molecular mechanism of BOD 2 and hydrogen peroxide reaction.

involves (i) singlet oxygen generated by BOD2, (ii) conversion of singlet oxygen to peroxide and (iii) reaction of peroxide with BOD2 to quench the activity is devised (Figure 3.3). Under cellular conditions, singlet oxygen is reported to transformed into less toxic reactive oxygen species such as hydrogen peroxide (H_2O_2) and since boronate moiety of BOD 2 is responsive to hydrogen peroxide (Xu et al, 2014), BOD 2 indirectly converts itself to BOD 1, a compound which does not generate singlet oxygen effectively. This unique reaction loop enables a smart control over photosensitizer BOD 2 activity.

Under photodynamic therapy singlet oxygen noted to be major ROS responsible for cytotoxicity. Convertion of $^1O_2$ to other, less reactive ROS are also studied. Accumulation of hydrogen peroxide is observed as a direct outcome of intracellular oxidation – reduction process (Kramarenko et al, 2016; Brilkina et al, 2018). Cells develop a defense mechanism againt overproduction of reactive oxygen species and tend to convert highly toxic intermadiates to less toxic kind through various antioxidant

Figure 3.3. Proposed mechanism of photodynamic activity control by feedback loop.

activity. One of the most well known antioxidant agent, ascorbate plays crucial roles in biological processes of cell such as photosynthesis, photoprotection, cell growth, and resistance to environmental stresses (Pshenichnyuk et al, 2016).
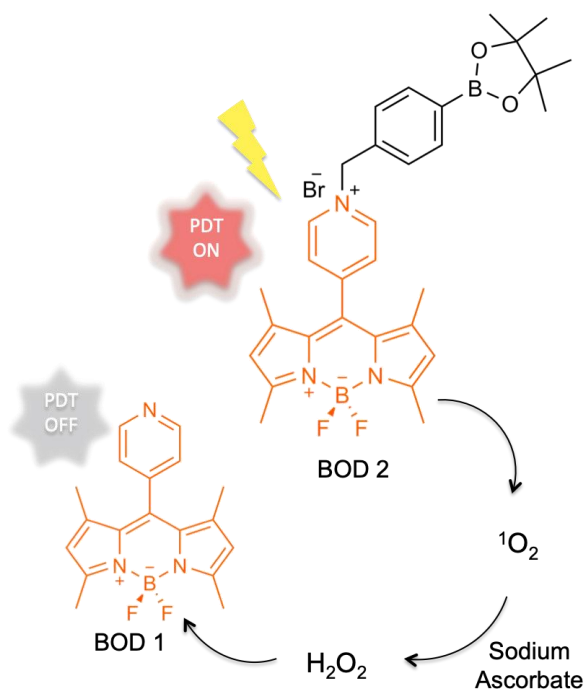
Moreover, ascorbate regulates particularly reactive oxygen species by catalysing the conversion of highly cytotoxic singlet oxygen ($^1O_2$) to H_2O_2 (Kramarenko et al, 2006). Singlet oxygen produced as a result of photodynamic action in living cells and used as therapeutic agent for cancer treatment (Li et al, 2016). In order to use intracellular redox chemistry for advanced control over photodynamic action, we take advantage of peroxide responsiveness of photosensitizer BOD 2 through incorporating boronate to BODIPY core. Designed photosensitizer produces $^1O_2$ under PDT and produced $^1O_2$ is transformed into H_2O_2 by means of ascorbate activity and accumulation of H_2O_2 inhibits photosensitizer action by a feedback loop (Figure 3.4). Reactive electrophilic singlet oxygen reacts rapidly with electron-rich moieties, ascorbate. And as a result of this reaction singlet oxygen ($^1O_2$) is generated by PDT reacts with ascorbate stoichiometrically to yield H_2O_2 (Kramarenko et al, 2006).
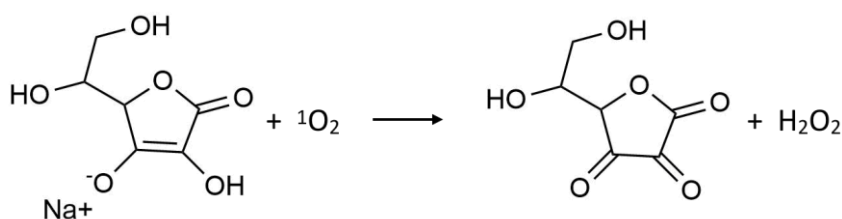
Figure 3.4. Reaction mechanism of sodium ascorbate with singlet oxygen. As a result of reaction ascorbate is converted into DHA, ketal form and hydrogen peroxide is produced from singlet oxygen.

In this account, designed molecule BOD 2 can produce both cytotoxic singlet oxygen when irratiated with light and PDT action is turned off upon generation of the hydrogen peroxide in time (Figure 3.5) Turning the activit of becomes possible for BOD 2 , since it react with the hydrogen peroxide particularly over other biologically relevant
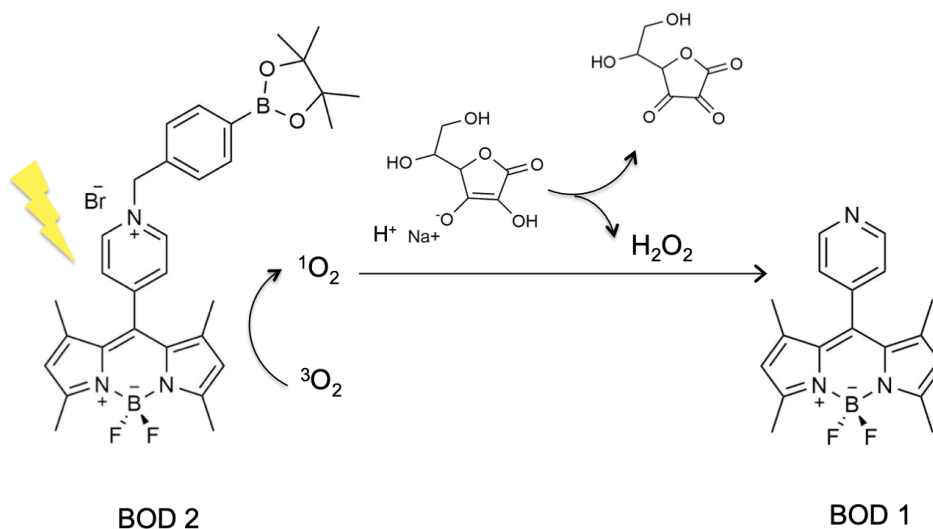
Figure 3.5. Feedback mechanism of target molecule BOD 2 presence of ascorbate.

ROS due to boronate moiety in the structure. In addition to activity control, this selective reaction also provide real time imaging of photosensitizer in both turn – on and turn – off mode by monitoring the enhancement of fluorescence intensity as BOD 2 is converted to BOD 1. In addition proposed activity control of BOD 2 meadiated through change in the chemistry of pyridinium moiety, compound tend to accumulate in mitochondria since pyridinium architecture provides a positive charge, yet lipophilic (Murphy, 2008). By means of cationic structure, designed molecule BOD 2 shows good solubility in water (Wang et al, 2009).

In the thesis, a photosensitizer is proposed with a novel singlet oxygen production approach, specific cellular localization and negative feedback control over the photodynamic action.

CHAPTER 4

RESULTS AND DISCUSSION

In the project a photodynamic agent with its boronate moiety in the structure is developed to have a negative feedback control over photodynamic action. The details of design and mechanism of feedback control is explained in Section 3. Photodynamic therapy agent is expected to have a feedback control through reaction with hydrogen peroxide. In order to understand the response of PDT agent to H_2O_2 two different experiments were done. In first of these experiment, peroxide response is monitored by change in fluorescence intensity (Figure 4.1).
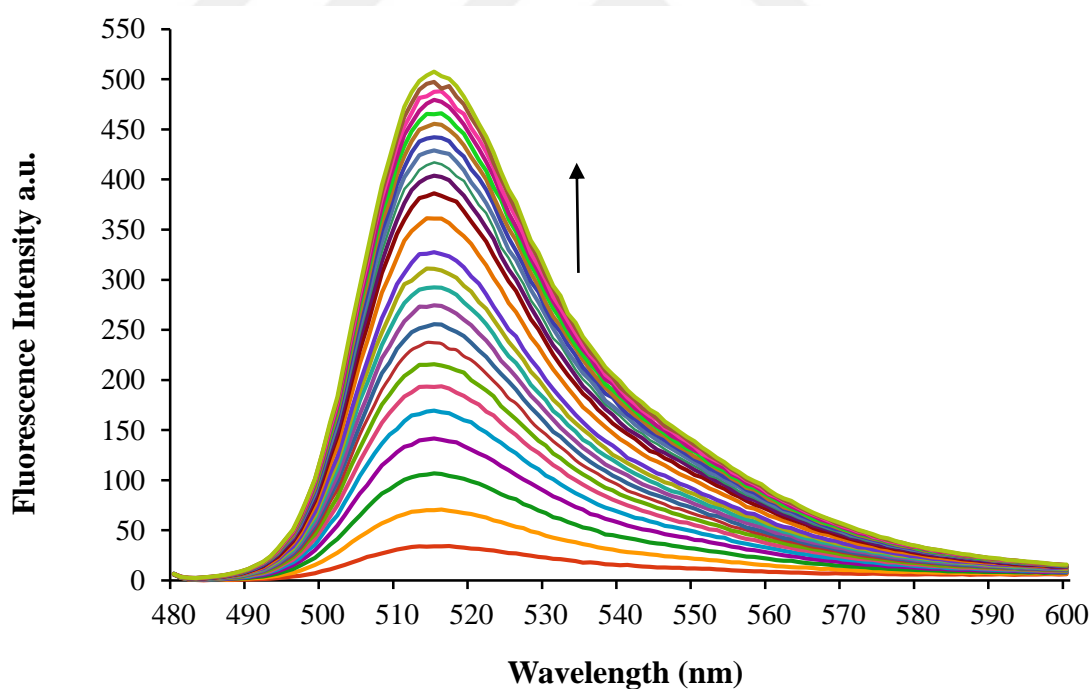
Figure 4.1. Fluorescence Spectra of BOD 2. Fluorescence turn-on response of 5 μM BOD 2 to 1 mM H_2O_2. Spectra shown were acquired after H_2O_2 addition (time up to 240 min). All measurements were acquired at 25°C in isopropanol within 10 min intervals, with $\lambda_{excitation}$ at 475 nm.

Upon addition of H_2O_2 (1 mM), the fluorescence of the BOD 2 (5 μM) gradually increased as time progressed as shown in Figure 4.1. The turn on fluorescence response reaches a platesu within 240 min (Figure 4.2). During the reaction with H_2O_2, the fluorescence intensity at 515 nm increased 15 fold of the initial value. This enhancement in fluorescence upon addition of peroxide proves that designed molecule BOD 2 can effectively respond to H_2O_2 through the release of boronate moiety as shown in Figure 3.2.
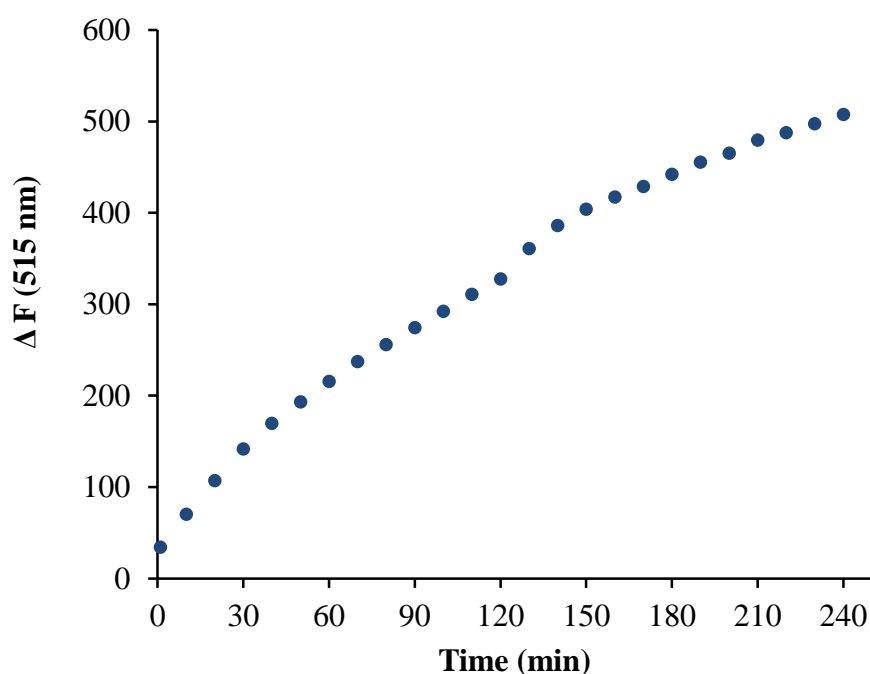
Figure 4.2. Fluorescence Spectra of BOD 2 at 515 nm. Measurement was acquired at 25°C in isopropanol within 10 min intervals, with $\lambda_{excitation}$ at 475 nm.

In order to further prove the reaction between BOD 2 and hydrogen peroxide an NMR experiment was performed. A solution of BOD 2 (10 mM) was prepared in NMR tube in dimethylsulfoxide (DMSO) and ^1H NMR is recorded. Changes in chemical shifts were recorded following the addition of H_2O_2 (10 M) in 30 minutes. Spectrums given in Figure 4.3. shows the formation of BOD 1 and byproduct which is 4-hydroxybenzyl

alcohol produced by 1,4-elimination reaction followed by addition reaction to double bond. Peaks b' resonating at 7.31 ppm corresponds to newly generated BOD 1 (Figure 4.3.a), peaks labelled as d' and f' with a chemical shift of 6.78 ppm, 5.76 ppm correspond to byproduct which starts to appear (Figure 4.3.a). BOD 2 peaks for pyridinium moiety (a and b) splits due to overelapping with the peaks corresponding to the intermediate boronic acid product as well as BOD 1.
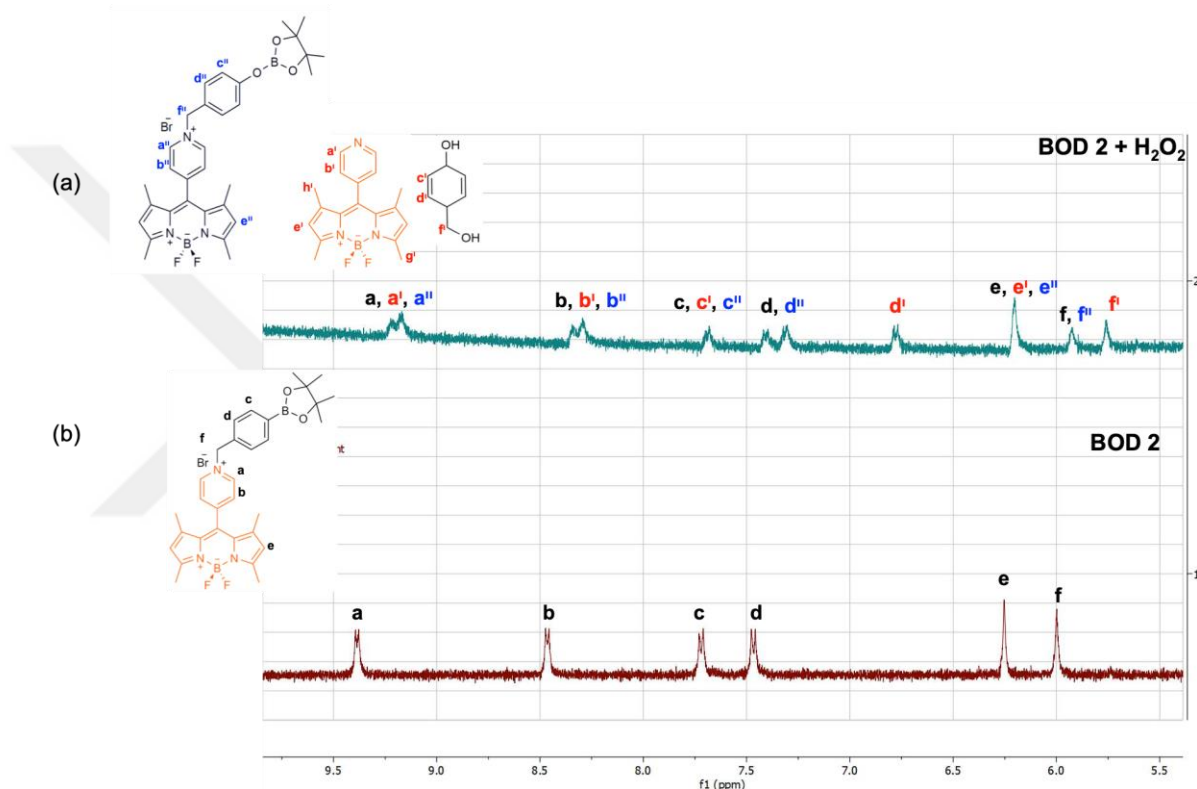
Figure 4.3.(a) ^{1}H NMR Spectra of BOD 2 30 minutes after the addition of 10M H_2O_2 (400 MHz, *d*-DMSO, 298K). (b) ^{1}H NMR Spectra of BOD 2 (400 MHz, *d*-DMSO, 298K). Peaks a', b' and f' corresponding to BOD1 and 4-hydroxybenzyl alcohol appears upon addition of peroxide.

^{1}H NMR experiments and fluorescence analysis prove the response of BOD 2 to peroxide. In agreement with literature data boronate group is sensitive to hydrogen peroxide and upon reaction fluorescent BOD 1 is generated (Xu et al, 2014).

In order to understand peroxide selectivity, fluorescence response of BOD 2 to various ROS is examined. Fluorescence turn-on response of 10 μM BOD 2 to 1 mM of each of tert – butyl hydroperoxide (TBHP), superoxide O_2^-, hypochlorite (OCl$^-$), tert – butoxy radical ($\cdot O^tBu$) and hydroxyl radical ($\cdot OH$) are analyzed and results are given in Figure 4.4.

1mM is far too high concentration for ROS other than H_2O_2, so if the photosensitizer do not display any response at this concentration it is expected to be less responsive in cellular media having lower ROS level. In Figure 4.4, each bar represent relative fluorescence response of agent to the labelled ROS 180 min after the addition of
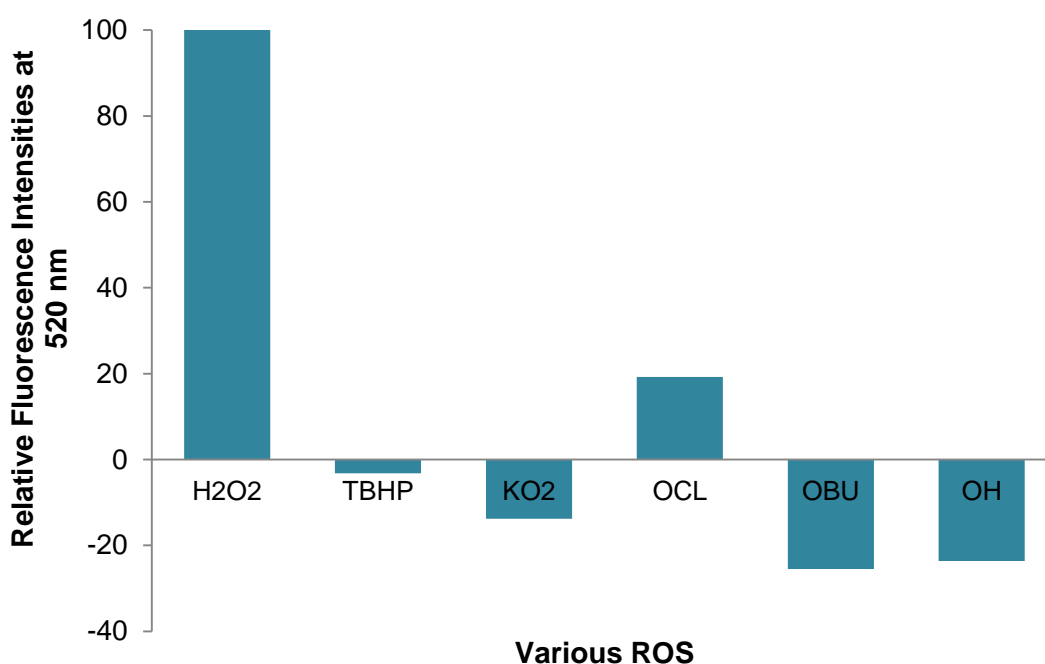
Figure 4.4. Relative fluorescence emission of BOD 2 180 min after addition of ROS. Fluorescence response of 10 μM BOD 2 is analysed using 1 mM of each of *tert* – butyl hydroperoxide (TBHP), superoxide O_2^-, hypochlorite (OCl$^-$), *tert*-butoxy radical ($\cdot O^tBu$) and hydroxyl radical ($\cdot OH$) hydroxyl radical ($\cdot OH$).

the given ROS. Emission was followed at 520 nm. Some of the ROS species (KO$_2$, $\cdot O^tBu$, $\cdot OH$, TBHP) display small decrease in fluorescene which is attributed to stability issues

of the agent under such high concentration of that ROS. Comparably smaller changes in fluorescent intensity proves that BOD 2 shows outstanding selective turn–on response to hydrogen peroxide. These results indicate that designed molecule BOD 2 show higher sensitivity and selectivity for hydrogen peroxide.

1,3-diphenylbenzofuran DPBF is used as a trap molecule to measure singlet oxygen production by PDT agent, since this compound is known to react selectively with singlet oxygen (Schmitz et al, 1982; Carloni et al,1993). In the presence of proposed photosensitizer and irradiation, the absorption of trap compound DPBF (yellow) decrease when it reacts with singlet oxygen and is decomposed to colorless 1,2 – dibenzoylbenzene. (Figure 4.5)
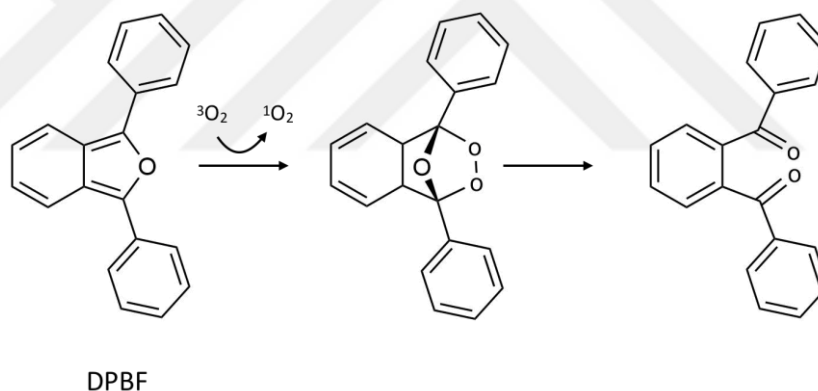
DPBF

Figure 4.5. Reaction of 1,3-diphenylisobenzofuran (DPBF) with singlet oxygen. In the project, change in the absorption spectra of DPBF as it reacts with $^1O_2$ is used to analyse PDT efficiency of agents.

Designed photosensitizer, BOD 2 (10 μM) was dissolved in isopropanol, due to insolubility of the trap molecule DPBF (50 μM) in water. DPBF alone, BOD 1 and BOD 2 samples was kept in the dark for the first 15 min then irradiated with 506 nm green LED

array for 80 min. Absorbance spectra were recorded at 5 min intervals. In the dark, presence of the designed molecule BOD 2 display no change in the absorbance of DPBF for 15 min indicating the absence of dark toxicity (PDT is only active when light is illuminated). On the other hand, when the sample is irradiated, there is prominent decrease in the absorbance of the trap molecule in the presence of BOD 2 due to rapid degradation with produced singlet oxygen (Figure 4.6). Following the green LED irradiation, the absorbance of DPBF at 411 nm decreased to one fifth of the original value.
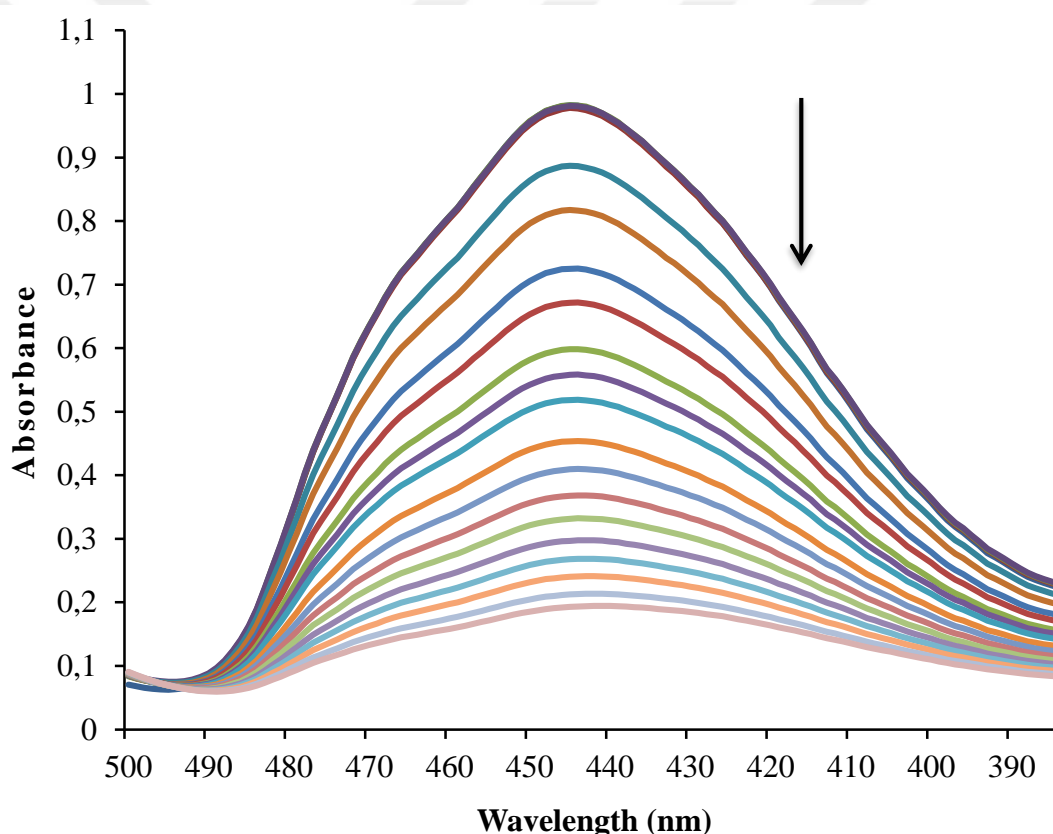
Figure 4.6. Change in absorbance Spectra of DPBF (50 µM) - BOD 2 (10 µM) under PDT. [1]O2 mediated photobleaching of 1,3-diphenylbenzofuran in isopropanol in the presence of 10 µM BOD 2 at room temperature. The sample was kept in the dark for the first 15 min and then irradiated with green LED array for 80 min (506 nm LED is used and the distance between light and the sample is 20 cm). First three spectra taken in the dark overlap.

This decrease proves that designed photosensitizer BOD 2 used effectively to produce singlet oxygen even though there is no heavy atom.

Control experiments are run without BOD 2 using same experimental conditions. In order to show that absorbance of the trap molecule DPBF does not decrease in the absence of the photosensitizer BOD 2 a separate experiment is done. Results are shown in Figure 4.7 and there is no change in absorbance of DPBF alone under same experimental conditions, whereas the sample that contains BOD 2 show substantial decrease in absorbance. Being the end product of the feedback control loop, photodynamic activity of BOD 1 is also analyzed. Although BOD 1 generates singlet oxygen to some extent under similar experimental conditions, this decrease in absorbance
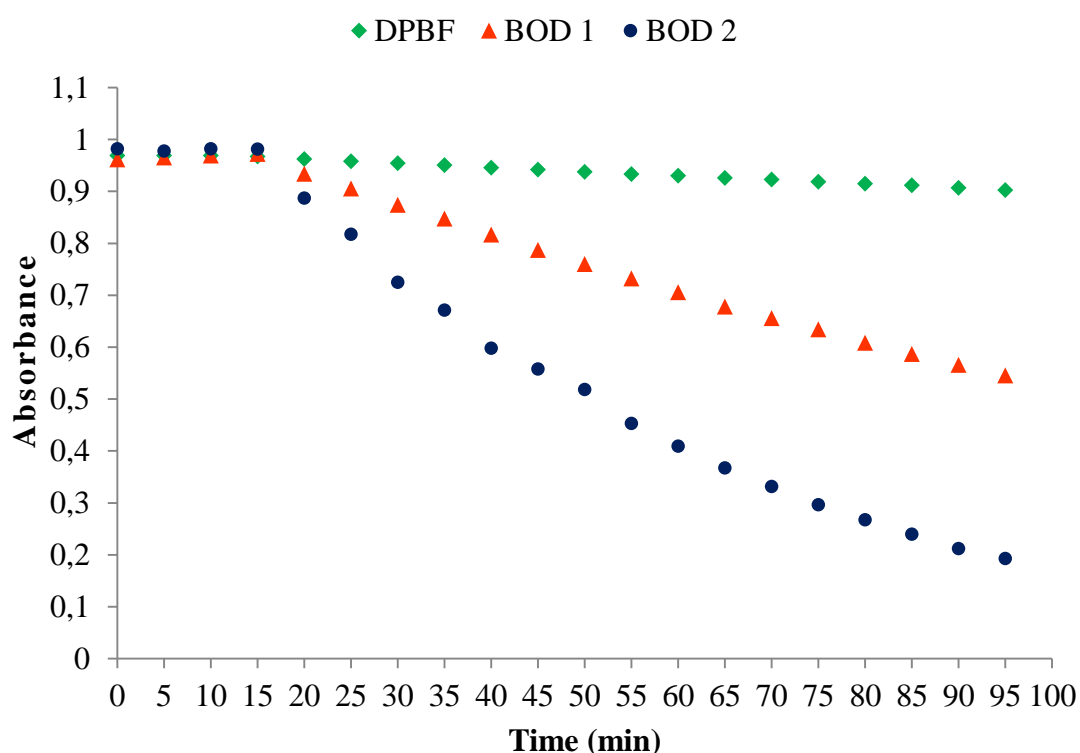
Figure 4.7. Singlet oxygen mediated photobleaching of DPBF with BOD 1 (10 µM), BOD 2 (10 µM) and DPBF (50 µM) in isopropanol as followed by absorbance change of DPBF at 411 nm. First 15 min spectra are recorded in the dark. For the rest samples are irradiated with 506 nm LED lamp.

of $^1O_2$ trap is far less efficient compared to photosensitizer BOD 2 consistent with the design. These experimental results indicate that when BOD 2 is converted to BOD 1, it will be in a form of less efficient PDT activity. In other words, photodynamic activity is reduced as BOD 2 is converted into BOD 1.

In this study designed compound BOD 2 is used as a photosensitizer and it shows efficient photo-induced singlet oxygen production even there is no heavy atom in the structure as opposed to pyridine bearing derivative BOD 1. Evidences show that designed photosensitizer has no dark toxicity at the concentrations used.

As a result of photodynamic action, desinged photosensitizer BOD 2 produce singlet oxygen effectively. As mentioned above singlet oxygen can be converted into hydrogen peroxide in the presence of ascorbate. Since BOD 2 is responsive to hydrogen peroxide, in order to measure the feedback loop (i.BOD 2 produces singlet oxygen; ii. singlet oxygen is converted to hydrogen peroxide by ascorbate; and iii. hydrogen peroxide reacts with BOD 2 to give fluorescent BOD 1) fluorescence spectra is recorded in the presence of ascorbate. As expeceted, in the presence of the all of BOD 2, ascorbate and irradiation, significant fluorescent increase is observed as shown in Figure 4.8 due to reaction of BOD 2 with hydrogen peroxide, the latter is produced from singlet oxygen of photodynamic action.

Fluorescence spectra were recorded at 10 min intervals for 240 min during irradiation at 506 nm green LED array from 10 cm distance. During the reaction with H_2O_2, the fluorescent at 518 nm showed significant increase and reaches more than five folds of the original value (Figure 4.8). Sample was kept in dark during the first 30 min, and no significant change in fluorescence intensity is observed during this period. This is an expected result, because in the dark no $^1O_2$ is produced and $^1O_2$ is necessary for H_2O_2 generation.
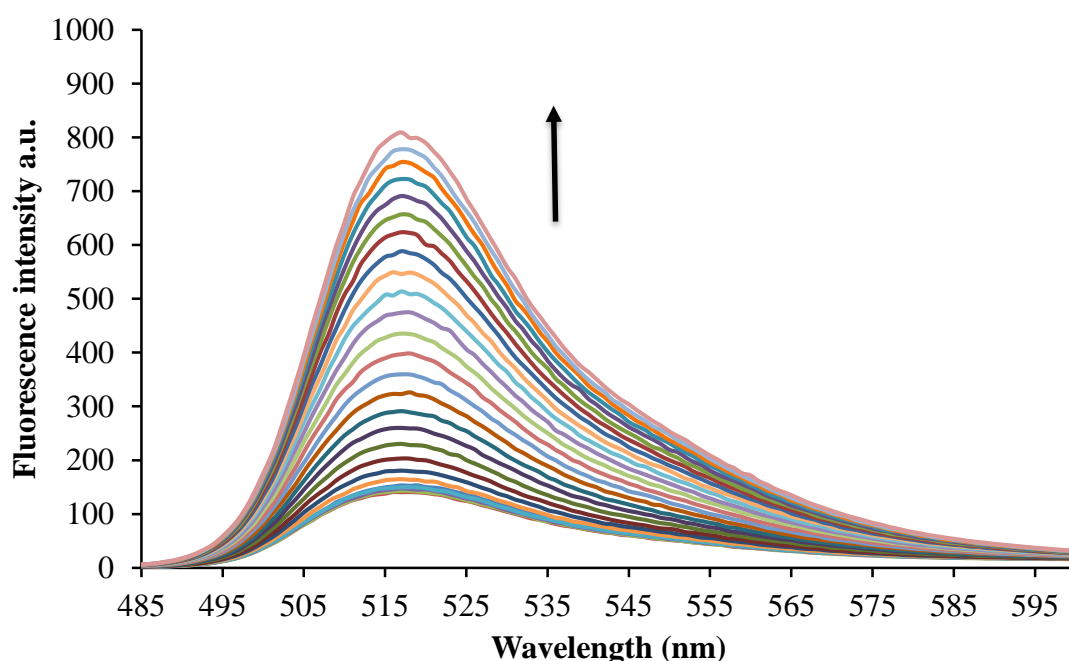
Figure 4.8. Fluorescence spectra of BOD 2 (10 µM) with sodium ascorbate (1mM). Fluorescence turn-on response to H_2O_2 produced from singlet oxygen were acquired after addition of sodium ascorbate. 506 nm green LED is used as source of irradiation from 10 cm distance. All measurements were acquired at 25°C in isopropanol within 10 min intervals, with $\lambda e_{xcitation}$ at 475 nm ($\lambda_{emission}$ interval: 465 – 600 nm). The first 30 min shows no apparent change in fluorescence intensity since these measurements were performed in the dark.
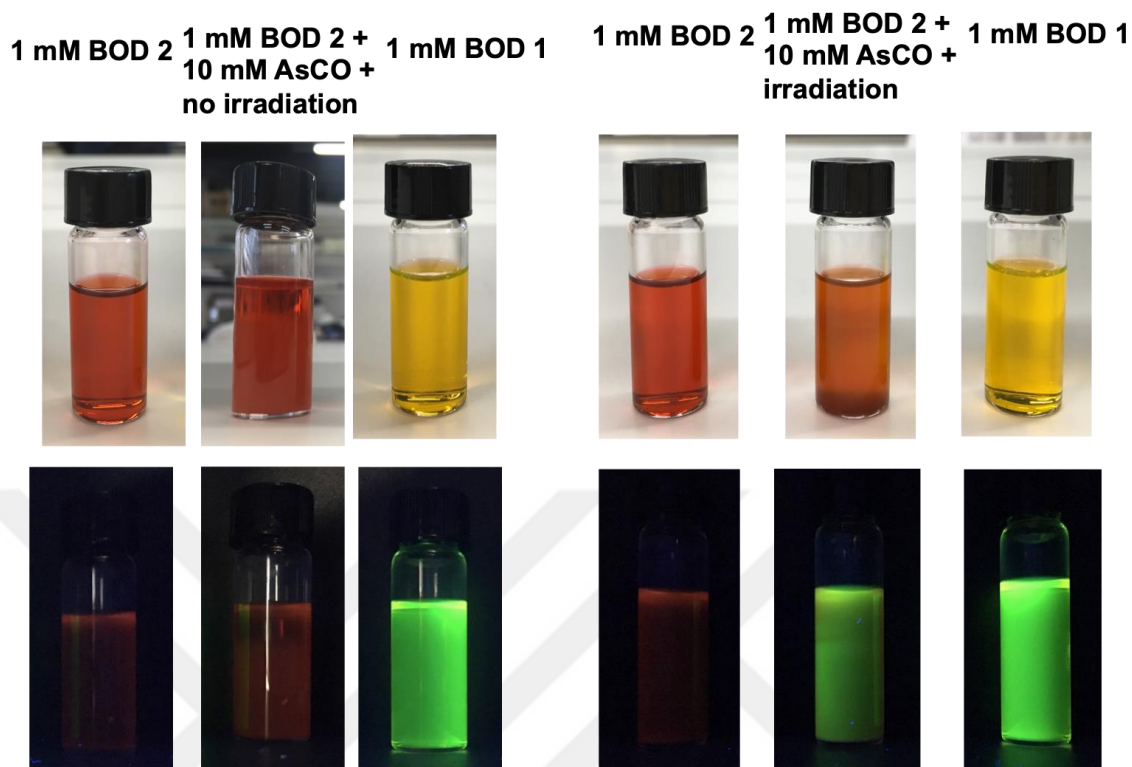
Figure 4.9. Photos of BOD 1 (1 mM) only, BOD 2 (1 mM) only and BOD 2 (1 mM) in the presence of sodium ascorbate (10 mM) and light. First group of pictures are taken prior to experiment. Fluorescence turn-on response to in situ produced H_2O_2 by the reaction with singlet oxygen were acquired after addition of sodium ascorbate. 506 nm green LED is used as source of irradiation from 20 cm distance for 180 min. All measurements were acquired at $25^{\circ}C$ in isopropanol.

Fluorescence turn – on response also proved perceptibly with BOD 2 (1 mM) in the presence of sodium ascorbate (10 mM) with 506 nm LED irradiation for 180 min. At the beginning, there is no fluorescence of BOD 2. After sodium ascorbate mediated reaction of singlet oxygen to produce H_2O_2 fluorescence of BOD can observed noticeably in Figure 4.9. In control experiment, there is no turn – on response of BOD 2 presence of sodium ascorbate due to lack of singlet oxygen generation with irradiation. Proposed mechanism of feedback control confirmed visibly.
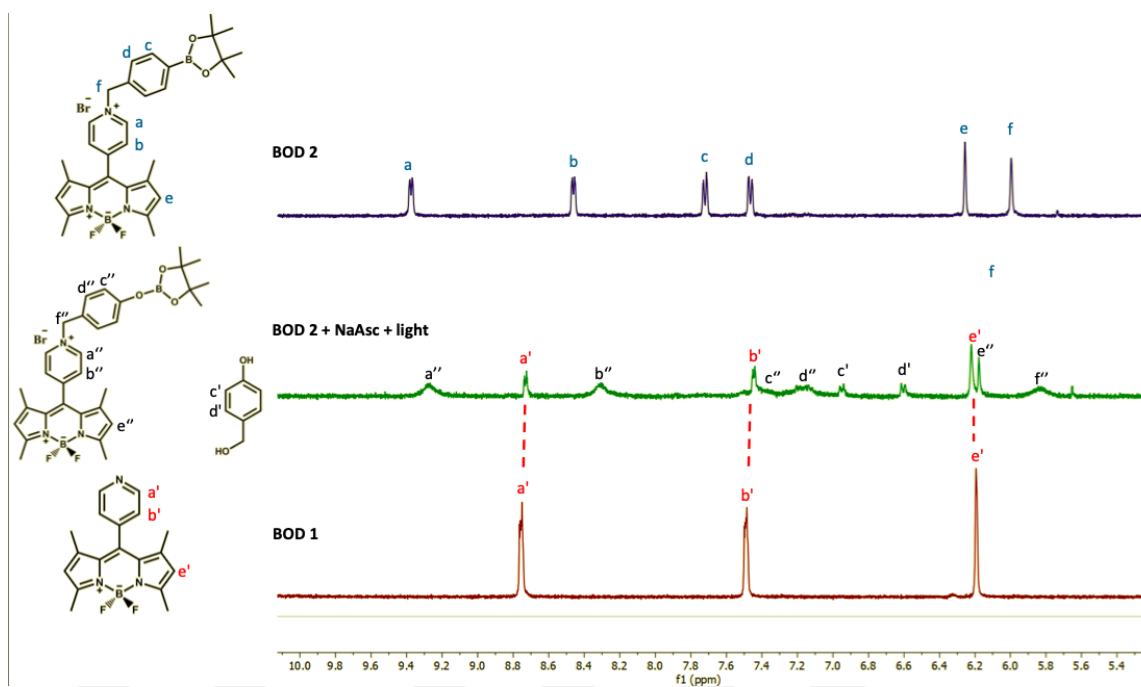
Figure 4.10.(a) ^{1}H NMR Spectra of BOD 2 (400 MHz, *d*-DMSO, 298K) (b) ^{1}H NMR Spectra of BOD 2 80 minutes after the addition of saturated sodium ascorbate (400 MHz, *d*-DMSO, 298K). (c) ^{1}H NMR Spectra of BOD 1 (400 MHz, *d*-DMSO, 298K)

In order to further confirm that irradiation of BOD 2 in the presence of ascorbate leads to conversion of BOD 2 to BOD 1, we performed an NMR analysis. BOD2 was irradiated with 506 nm light for 80 min in the presence of saturated ascorbate solution and it has been shown that BOD1 peaks appears while BOD 2 peaks disappear (Figure 4.10). Signal corresponding to first oxidation product and elimination product also appears, which are all assigned in the spectrum. This result directly demonstrate the formation of BOD 1 from BOD 2 under the proposed conditions.

Control experiments is performed under same experimental conditions. Looking at singlet oxygen production experiment of BOD 1, the fluorescence increase in the presence of in situ generated H_2O_2 (produced from sodium ascorbate and singlet oxygen reaction) is far less than photosensitizer BOD 2 (Figure 4.11). Since there is no boronate ester in the structure of BOD 1 to be cleaved by peroxide, this fluorescence enhancement may be attriuted its interaction with ascorbate. Since the mechanism of this small fluorescence enhancement is beyond the subject of the thesis, no further analysis is performed with BOD 1.
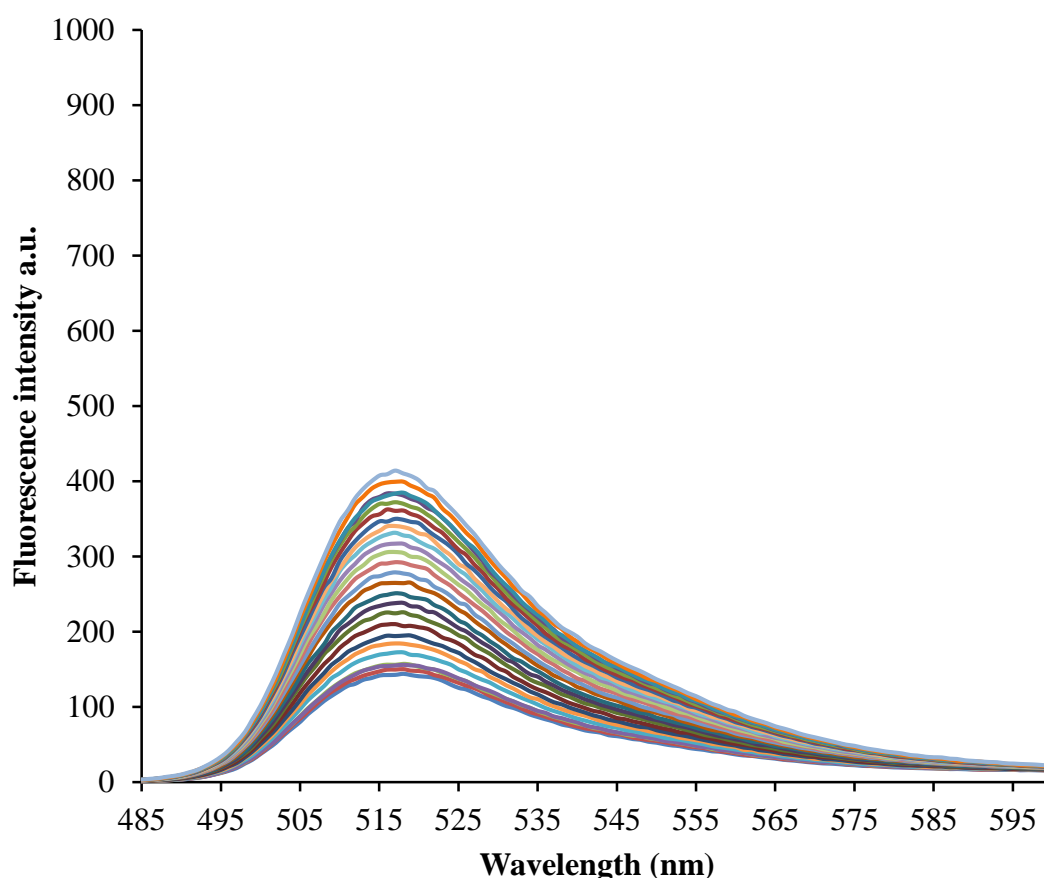
Figure 4.11. Fluorescence spectra of BOD 1 (10 μM) in the absence of sodium ascorbate. 506 nm green LED is used source of irradiation from 10 cm distance for photodynamic action following 30 min dark period. All measurements were acquired at 25°C in isopropanol within 10 min intervals, with $\lambda_{excitation}$ at 475 nm ($\lambda_{emission}$ interval: 465 – 600 nm).

Results shown in Figure 4.12 indicates that in the absence of the sodium ascorbate, produced singlet oxygen can not be converted into hydrogen peroxide, and as expected, flurorescence increase is less in the sample that lack ascorbate compared to one with sodium ascorbate. The feedback loop experiments proves that designed photosensitizer BOD 2 displays precise control over production of cytotoxic singlet oxygen generation. Above findings suggest that once photosensitizer is irradiated with light, produced singlet oxygen reacts with sodium ascorbate in the cell generates hydrogen peroxide. In return, as proved by fluorescent response experiments (Figure 4.8 and 4.11), BOD 2 reacts with hydrogen peroxide, regain its fluorescence and produce less efficient BOD 1 agent. Altogether, proposed study may offer a novel methodology for self feedback- controlled photodynamic action with a simple and biologically relevant components.
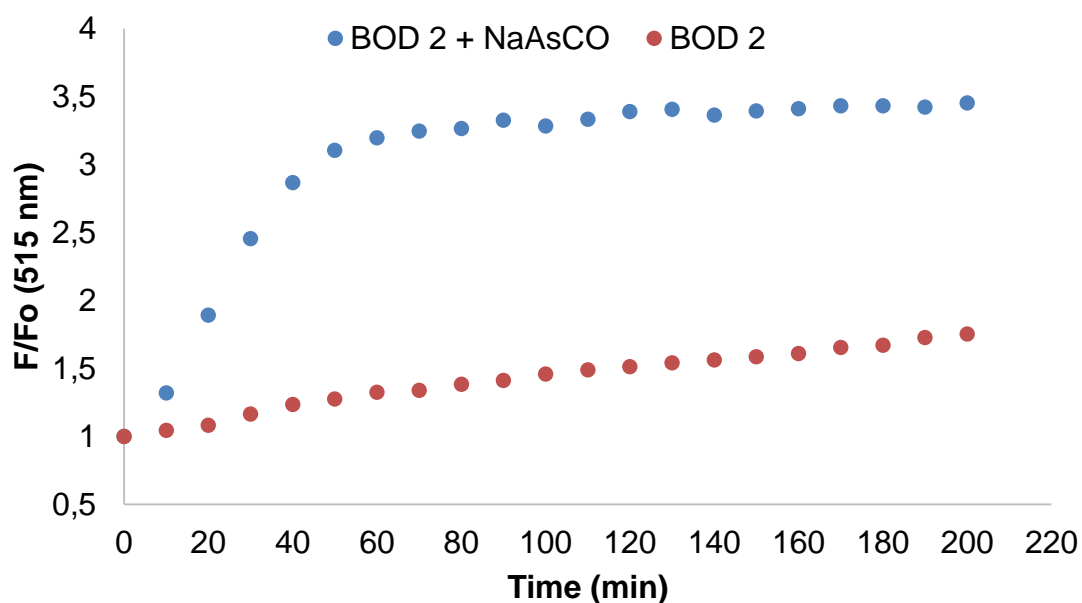
Figure 4.12. Fluorescence spectra of BOD 2 alone (10 μM) and BOD 2 (10 μM) with sodium ascorbate (1mM) at 518 nm. Sample is kept in dark during first 30 min and irradiated with 506 nm LED light source. All measurements were acquired at 25°C in isopropanol within 10 min intervals, with $\lambda_{excitation}$ at 475 nm ($\lambda_{emission}$ interval: 465 – 600 nm).

As an another evidence shown Figure 4.13, efficiency of DPBF reaction with photo – induced generated singlet oxygen decreased in presence of the ascorbate as expected. As a result of reaction between ascorbate and singlet oxygen, hydrogen peroxide produced and inhibited the photodynamic action. Additionally, decrease in absorbance of DPBF matching with concentration of ascorbate (0, 0.2 mM and 1 mM ascorbate) compared in Figure 4.13. The fast response to high concentration of ascorbate result in consumption of generated singlet oxygen and competes with the reaction DPBF.
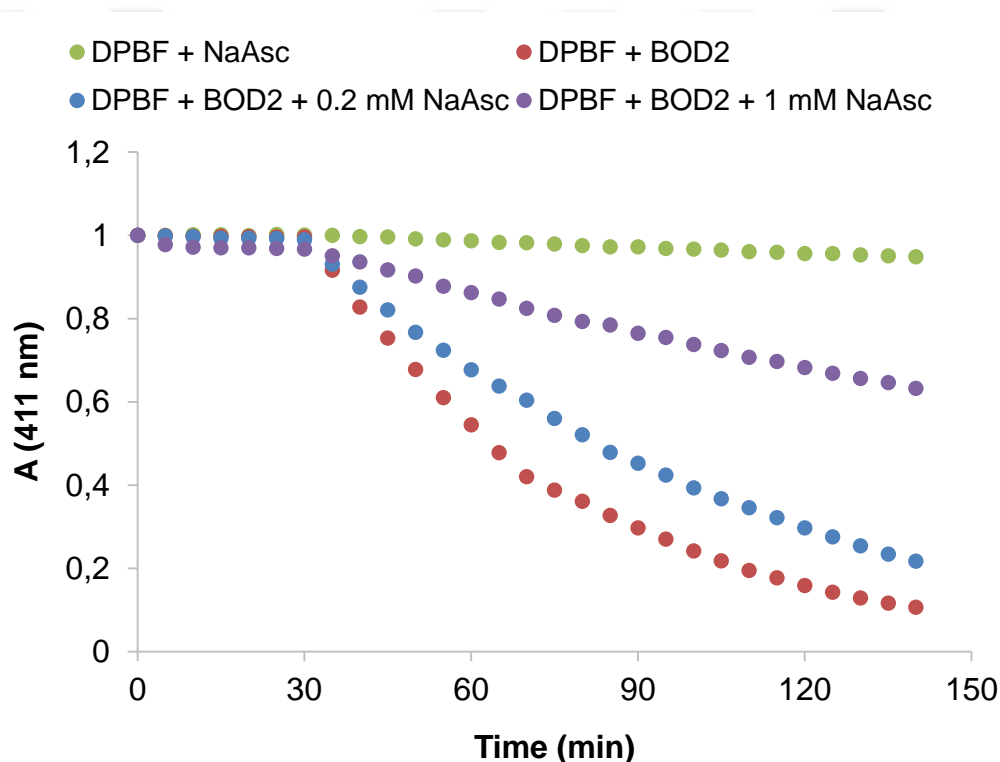
Figure 4.13. Absorbance spectra of DPBF (10 μM) in the presence of ascorbate only (green), 0.2 mM ascorbate and 10 μM BOD 2 (purple), 1mM NaAsc and 10 μM BOD2 (blue) and in the presence of 10 μM BOD 2. Sample is kept in dark during first 30 min and irradiated with 506 nm LED light source. All measurements were acquired at 25°C in isopropanol within 10 min intervals.
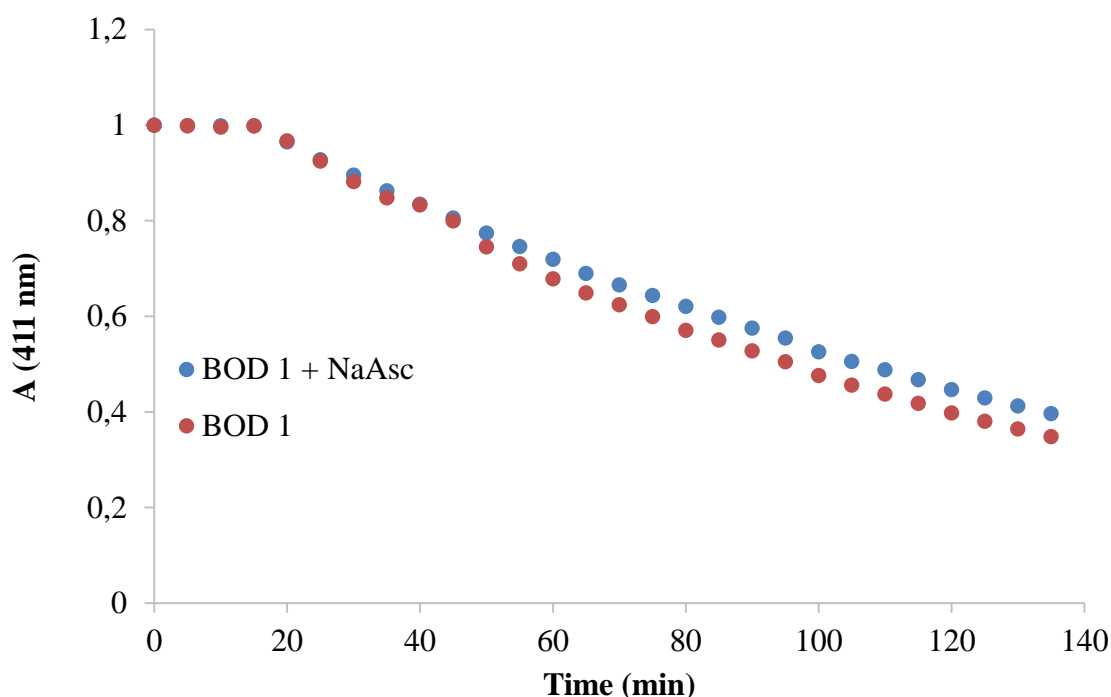
Figure 4.14. Absorbance spectra of DPBF (50 μM) in the presence of 0.2 mM ascorbate and 10 μM BOD 1 (blue) and in the presence of 10 μM BOD 1 (red). Sample is kept in dark during first 30 min and irradiated with 506 nm LED light source. All measurements were acquired at 25°C in isopropanol within 10 min intervals.

Herein, BOD 1 were tested as $^1O_2$ sensitizer for photooxidation of DPBF presence of sodium ascorbate. Since BOD 1 is not efficient photodynamic agent as much as BOD 2, decrease in time is not notable. Moreover, in this experiment effect of sodium ascorbate on BOD 1 examined during photobleaching of DPBF demonstrated in Figure 4.14. Previously shown in Figure 4.7 and 4.11, BOD 1 is not potential agent for photodynamic therapy in the way of singlet oxygen generation. Additionally, there is also no response to hydrogen peroxide due to lack of boronate moiety. As a result of this control experiment, it has been shown that effect of ascorbate on PDT action is not removal of oxygen from the solution but through feedback loop, decrease the concentration of BOD 2 in the media.

User Spectra

Fragmentor Voltage	Collision Energy	Ionization Mode
60	0	APCI

+APCI Scan (rt: 0.144 min) Frag=60.0V mmy-12.d

Counts vs. Mass-to-Charge (m/z)
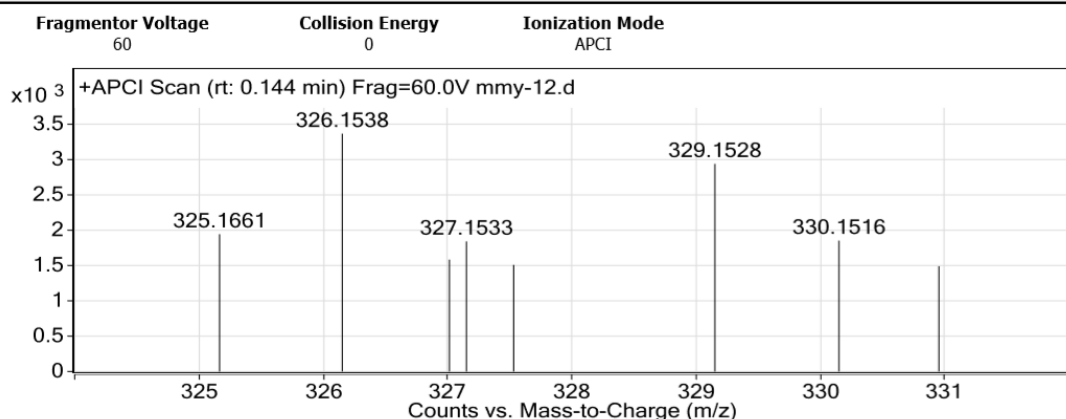
Figure 4.15. High resolution ESI-MS spectrum of BOD 2 (10 μM) with sodium ascorbate (0.2 mM). Reaction based turn-on response tested to H_2O_2 produced from singlet oxygen were acquired after addition of sodium ascorbate. 506 nm green LED is used as source of irradiation from 20 cm distance for 150 min. All measurements were acquired at $25^{o}C$ in isopropanol. m/z peak corresponding to BOD1 indicates the formation of this species during PDT action. (M+H)+ theoritical: 326.1640; experimental:326.1538; Δ: 31 ppm.

HRMS spectra of BOD 2 was recorded in the presence of 0.2 mM sodium ascorbate after irradiation with 506 nm LED light source for 150 min. In addition to the proof obtained by spectrophotometric characterization of BOD 1 formation from BOD 2 during PDT action, mass analysis after PDT action shown in Figure 4.15 demonstrate the presence of peaks corresponding to BOD 1. HRMS results provide perceptible evidence for proposed feedback control mechanism through which inactive BOD1 is generated. Formation of BOD 1 is evident through appearance of BOD 1 peaks as a result of sodium ascorbate mediated reaction of singlet oxygen to produce H_2O_2.

Further photophysical characterization of proposed feedback mechanism determine with quantum yield measurement. The results shown in Table 4.1 indicate that

presence of sodium ascorbate and light the value of the quantum yield get closer from

BOD 2 to BOD 1.

Compound	$\lambda_{max, abs}$ (nm)	$\lambda_{max, fluo}$ (nm)	ϕ_F
BOD 2	510	515	0.04
BOD 2 + NaAsc + Light	505	515	0.16
BOD 1	504	515	0.31

Table 4.1. Photophysical properties of BOD1, BOD2 and BOD2 in the presence of 0.2 mM sodium ascorbate irradiated with 506 nm light for 150 min. All measurements were obtained in isopropanol.

It has been proposed spectrophotometric and chemical properties of compound BOD 2. Here, Figure 4.16 focuses effects of pH on chemical stability of BOD 2. The experiment conducted in two different pH buffer solution (pH 6.0 and pH 7.2) and fluorescence results recorded at 511 nm for 60 hours. The pH stability graph in Figure 4.16 proved that BOD 2 exhibit remarkable stability at biological pH range. Fluorescence change is not noticeble until 24 h and all experiments completed within this time.
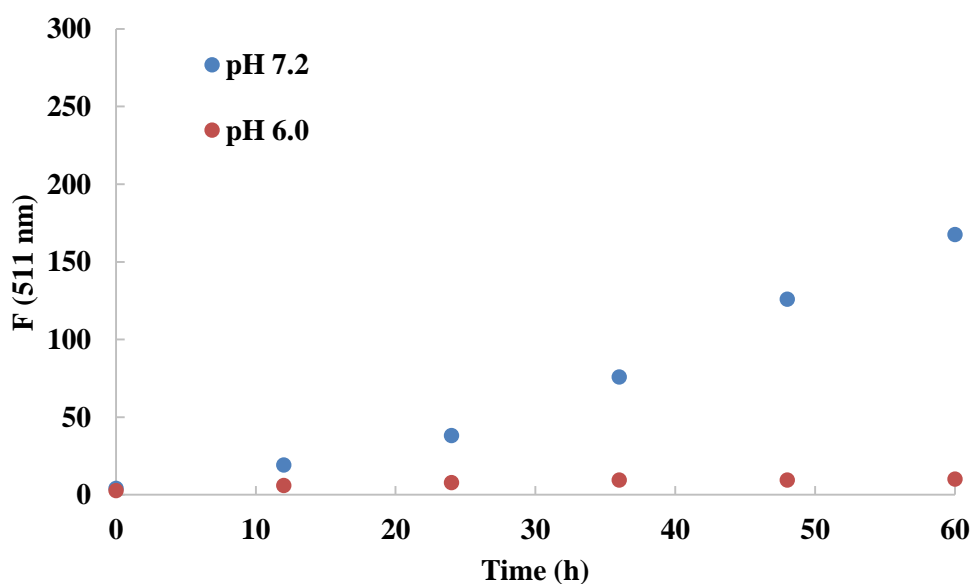
Figure 4.16. Stability of BOD 2 (5 µM) in PBS buffer at pH 7.2 and pH 6.0. All measurements were acquired at 25°C in isopropanol within 12 hours intervals for 60 hours, with $\lambda_{excitation}$ at 475 nm.

Literature based studies demonstrate that microenvironment of tumor tissue is often acidic as a result of acidic metabolites like lactic acid e.g.(Warburg et al, 1924). The Warburg effect is widely popular theory about extracellular acidity of tumor environment. These results provide further data for BOD 2 highly stable even acidic condition like tumor cells.
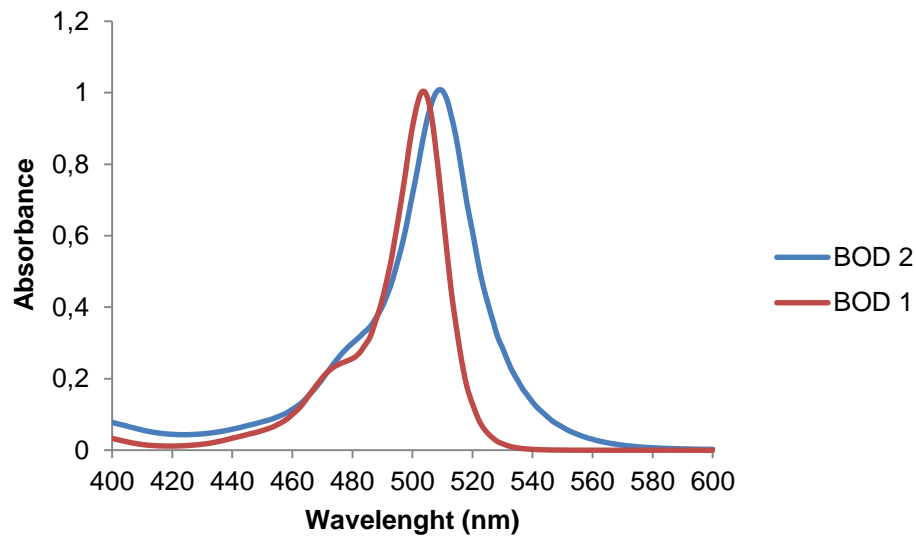
Figure 4.17. Normalized absorbance spectra of BOD 1 and BOD 2. All measurements were acquired at 25°C in isopropanol.
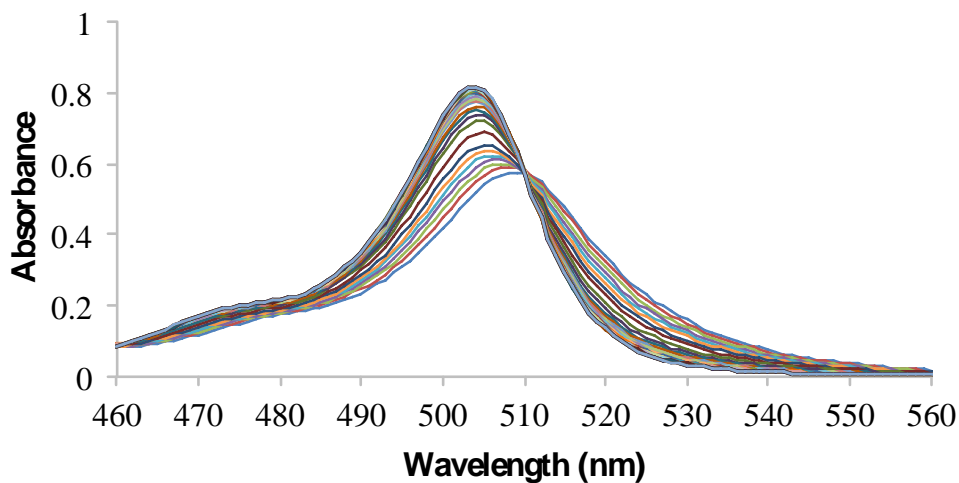
Figure 4.18. Time dependent changes in absorbance of BOD 2 during PDT action. Sample is kept in dark during first 30 min and irradiated with 506 nm LED light source. All measurements were acquired at 25°C in isopropanol within 10 min intervals.

Time dependent changes in absorbance and fluorescence increase prove that BOD 2 turn into BOD 1 during the photodynamic action. Ratio of absorption spectral shift of BOD 2 from 505 nm to 510 nm demonstrated in Figure.4.19 (dark) and Figure.4.20 (light). Gradual increase in the absorption peak corresponding to BOD1 is increased upon irradiation whereas in the dark a small increase in the ratio is observed which is attributed to anion change from bromide to acetate.
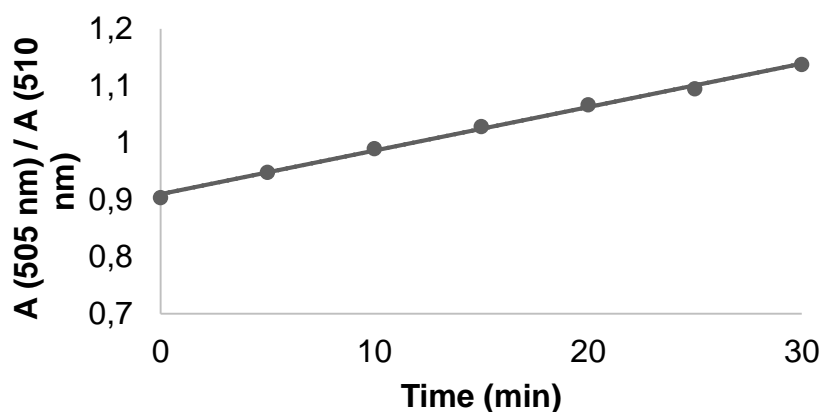
Figure 4.19. Ascorbate dependent change in ratio of absorption at 505 nm to 510 nm in the dark before irradiation.
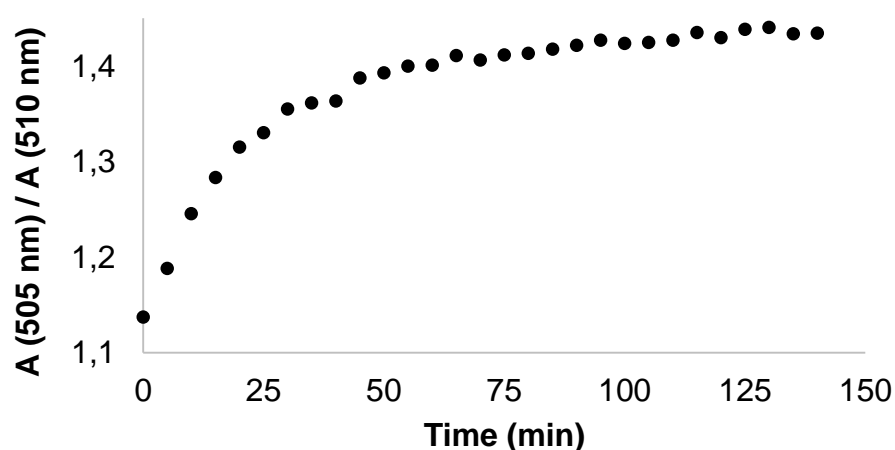
Figure 4.20. Ascorbate dependent change in ratio of absorption at 505 nm to 510 nm in the presence of light.

The elucidation of tumor cells has tendency to metastasis has been major problem of cancer research. Particularly, colorectal cancer (CRC) types show metastatic spread characteristic and among the other cancer types placed in fourth as most common causes of cancer mortality (Portera et al 1998; Wen et al, 2007). By nature of invasive tendency of such cancer types, chemotherapy has been only modality for treatment. On the other hand, over the other traditional methods PDT induce cancer treatment with minimal doses, non – invasive feature, repeated application and certain localization even at subcellular parts such as mitochondria, lysosome or plasma (Kessel and Oleinick, 2009). In the present study, efficacy of BOD 2 on photo – induced cell death is demonstrated.

The in vitro cell experiments carried out on human colorectal adenocarcinoma cell line DLD – 1 for verification of fluorescence response and photodynamic action. Cell suspension of DLD – 1 human colorectal adenocarcinoma cell were prepared in T – 75 culture flaks within RPMI 1640 culture medium at $37^{o}C$ in a humidified incubator containing %5 CO_2. After incubation, for cell viability testing, standard alamarBlue assay performed. IC_{50} test results proved that the cell can internalize heavy-atom free
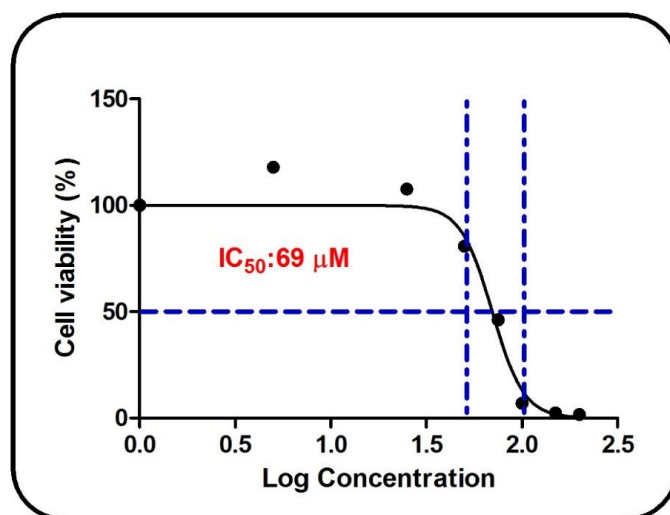
Figure.4.21. Concentration dependence of cell viability. Half maximal inhibitory concentration (IC_{50}) of BOD 2.

photosensitizer with no apparent toxicity (IC_{50} is 69 μM) in the concentration range applied. Concentration dependent cell viability spectrum is displayed in Figure 4.21.

For fluorescence imaging of H_2O_2 response of BOD 2, DLD – 1 seeded aforementioned procedure. Following steps conducted; cells treated with 10 μM H_2O_2, medium washed with PBS, dyed with MitoTracker (to stain mitochondria) and after washing, 5 μM BOD 2 administered. After incubation with BOD 2, the cells were washed with PBS buffer and visualized with fluorescent microscope at 20x and 80x. images were taken at green wavelength. As expected, due to cationic and lipophilic structure of BOD 2 localized in mitochondria (Figure 4.22)
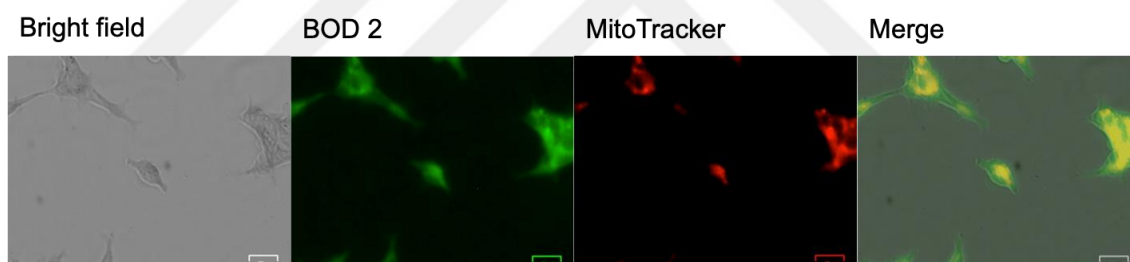
Figure 4.22. Fluorescence imaging of DLD – 1 cells.

Most of PDT agent contains heavy atom to facilitate intersystem crossing by spin - orbit coupling (Kamkaew et al, 2013). Heavy - atom incorporated agents may have biological intolerance, and also can cause dark - toxicity (Eckl et al, 2017). Unlike traditional PDT agents, designed photosensitizer BOD 2 is heavy - atom free and does not show dark - toxicity at cellular and sub - cellular levels as proved cell viability test. For testing phototoxic activity of BOD 2, DLD – 1 cells were cultured before mentioned protocol. After incubation, RPMI 1640 medium renewed with the medium containing 10

µM BOD 2. Cells irradiated with green LED array (506 nm) source from 8 cm for 2 hours. Control groups are defined as; cell viability examined under dark and light condition without PDT agent and tested photocytoxicity of the final product of feedback loop, BOD 1 in dark and light. As a result of photodynamic action BOD 2 induced cell death successfully when light applied shown in Figure.4.23.

There is a significant difference between dark and light condition of BOD 2 as predicted. Photocytotoxicity of control groups proved that applied light do not effect cell viability and BOD 1 shows no significant result in the way of photodynamic action. This result also proved proposed feedback control over photodynamic action with in vitro assay. For further studies specially in vivo and clinical applications, this research will be proof of concept.
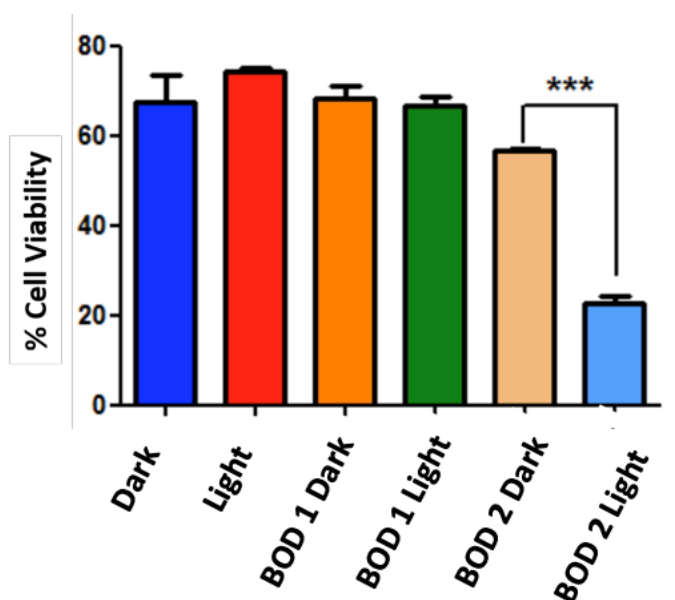
Figure 4.23. Phototoxicity of BOD 1 and BOD 2 in presence and absence of the light.

CHAPTER 5

EXPERIMENTAL SECTION

5.1. Fluorescence Measurement of BOD 2 with H_2O_2

All spectroscopic measurements were performed in isopropanol at room temperature. UV – Fluorescence spectral studies performed using Agilent Technologies Cary 60 UV-Vis and Agilent Technologies Cary Eclipse with Xenon Flash lamp. Samples for absorption and fluorescence measurements were contained in 1 cm x 1 cm quartz cuvettes.

For fluorescence experiment, 15 mg (25 μmol) BOD 2 is dissolved in 5 ml isopropanol and 5 mM BOD 2 stock solution is prepared. 5 mM BOD 2 solution was first diluted to 200 μM concentration of second stock solution. Then appropriate amount of BOD 2 from stock solution (200 μM) and H_2O_2 stock solution (100 mM) mixed in a cuvette such that the final calculated concentration of BOD 2 is 5 μM and H_2O_2 is 1 mM. Hydrogen peroxide was used from commercial %30 w/w solution. The fluorescent spectra were recorded with Agilent Technologies Cary Eclipse right after addition of H_2O_2 for 240 min. The fluorescence changes of the BOD 2 in presence of H_2O_2 monitored by spectrophotometer within 10 min intervals. Excitation wavelength was at 475 nm and emission was followed between the wavelengths of 465 – 600 nm.

5.2. ^{1}H NMR Experiment

10 mM BOD 2 was dissolved in NMR tube in dimethylsulfoxide (DMSO) and ^{1}H NMR is recorded. After 30 min from addition of 10 M hydrogen peroxide, chemical shifts were observed.

5.3. ROS Selectivity Experiments

For selectivity experiments, the fluorescence response of BOD 2 to common reactive oxygen species (ROS) examined. In the sample cuvette, the final concentration of BOD 2 was 10 μM and various ROS was 1 mM. ROS analysed in the experiment were H_2O_2, tert-butyl hydroperoxide (TBHP), superoxide (O_2^-), hypochlorite (OCl^-), tert-butoxy radical ($\cdot O^tBu$) and hydroxyl radical ($\cdot OH$). Final solution of H_2O_2, TBHP and OCl^- were 1 mM and all were prepared by dilution from commercial bottle. Superoxide ($O_2^{\cdot-}$) solution was prepared from potassium superoxide (KO_2) salt in water. Hydroxyl radicals ($\cdot OH$) and tert-butoxy radical ($\cdot O^tBu$) were generated using the reaction of H_2O_2 with Fe^{2+} (Iron (II) sulfide) as described in literature (Chung et al,2011)

The fluorescence spectra were recorded after addition of ROS for 180 min. The fluorescence changes of the BOD 2 in presence of ROS monitored by fluorescence spectrophotometer (Bio Tek Microplate Spectrophotometer) with excitation wavelength at 475 nm whereas emission is followed between 465 – 600 nm.

5.4. Singlet Oxygen Generation Experiments

For measurement of singlet oxygen generation, $^1O_2$ dependent degradation of the trap molecule 1,3-diphenylbenzofuran (DPBF) is analyzed and used as a measure of

photodynamic activity. Absorption of this trap compound at 411 nm in isopropanol decreases as generated $^1O_2$ reacts with DPBF. Corresponding reaction is given in Figure.4.5 Final solutions in cuvettes contains DPBF (50 μM), BOD 1 (10 μM) and BOD 2 (10 μM), all prepared in isopropanol. 506 nm green LED (LED from Bright LED Electronics Corp. and model BL-BG43V4V with peak absorption value at 506 nm was used as a light source) is used for irradiation from 20 cm. Two control solution: DPBF alone (50 μM) and DPBF (50 μM) with BOD 1 (10 μM) are used to compare activity of proposed photosensitizer. The samples were kept in the dark for the first 15 min then irradiated at 506 nm green LED array for 80 min. Absorbance spectra were recorded at 5 min intervals. The decrease in absorbance of DPBF at 411 nm enables comparison of singlet oxygen production efficiencies of model and designed compounds BOD 1 and BOD 2 respectively.

5.5.   Measurement of BOD2-$^1O_2$-Ascorbate-H_2O_2-BOD1 Loop Formation

For feedback loop experiments, the final concentrations of BOD 1 and BOD 2 were diluted to 10 μM from stock solution separately. Sodium salt of ascorbate (SA) is synthesised by mixing 10 mmol ascorbic acid (AA) and 10 mmol sodium bicarbonate (NAHCO$_3$) in methanol at 55°C. Then the product is precipitated. Crystals are collected via filtration and dried in oven. In cuvettes, the final concentration of BOD 1 and BOD 2 was 10 μM and sodium ascorbate was either 0, 0.2 or 1 mM. The fluorescent spectra were recorded right after addition of sodium ascorbate for 240 min. For singlet oxygen generation, 506 nm green LED is used as a source of irradiation from 10 cm distance. The fluorescence changes of the BOD 1, BOD 2 in presence of sodium ascorbate were monitored by fluorescence spectrophotometer within 10 min intervals, with excitation wavelength at 475 nm whereas emission interval was 465 – 600 nm.

5.6. ^{1}H NMR Loop Experiment

25 mM BOD 2 was dissolved in NMR tube in dimethylsulfoxide (DMSO) and ^{1}H NMR is recorded. After from addition of saturated sodium ascorbate, sample was irradiated with 506 nm LED array during 80 min. formation of BOD 1 from BOD 2 presence of ascorbate and irradiation recorded.

5.7. High Resolution ESI-MS Spectrum Loop Experiment

BOD 2 (10 μM) with sodium ascorbate (0.2 mM) dissolved in test cuvette. Reaction based turn-on response tested to H_2O_2 produced from singlet oxygen were acquired after addition of sodium ascorbate. 506 nm green LED is used as source of irradiation from 20 cm distance for 150 min. All measurements were acquired at 25°C in isopropanol.

5.8. Quantum Yield Experiment

Quantum yield calculation were done using standard chromophore Rhodamine G6 (excitation wavelenght at 488 nm in water) having quantum yield 0.95. In order to prevent self – quenching, all absorbance values adjusted below 0.1. Following formula used for calculation of quantum yield of BOD 1, BOD 2 and BOD 2 presence of sodium ascorbate and light: (Lakowicz, 2010)

$$Q = Q_R \, (I/I_R) * (A_R/A) * (n^2/n_R^2)$$

Q_R strands for quantum yield of reference, I and I_R integrated area of emission spectrum both for sample and and reference, A and A_R refer to absorbance of sample and reference at corresponding wavelenght (at 488 nm), n and n_R (1.333 for water and 1.3776 for

isopropanol) represents refractive indices of solvent in which sample and referance compound dissolved. All samples BOD 1, BOD 2 and BOD 2 with sodium ascorbate dissolved in isopropanol and refernce Rhodamine G6 dissolved in water.

5.9. Stability Experiment

Buffer solutions were prepared with phosphate buffered saline (PBS) tablet (Sigma 4417). The tablet was dissolved in 200 ml ultra pure water and pH is adjusted to 7.2 and 6.0 using HCl and NaOH. BOD 2 added fluorescence cuvette and final concentration of BOD 2 was 5 micromolar. During 60 hours, cuvettes were kept in the dark.

5.10. Cell Experiment

Cell culture experiments were run in Department of Biochemistry, Selçuk University. DLD – 1 human colorecral adenocarcinoma cells (ATCC) were cultured in T – 75 culture flaks within RPMI 1640 culture medium at 37°C in a humidified incubatorcontaining %5 CO_2 (Binder Series CB | CO_2 incubators). The standard RPMI medium supplemented with heat – inactived 10% fetal bovine serum, 2 mM L – glutamine, 100 units mL^{-1} penicilin G and 100 μg mL^{-1} streptomycin at 37 °C in a humidified incubator containing %5 CO_2. After incubation of cell line for 24 h, medium washed with PBS buffer and cell viability tested with 0 – 200 μM concentration range of BOD 2 in 24 well plate containing 10^6 cell/well. For cell viability testing, standard alamarBlue (ThermoFisher) assay performed. The resazurin (alamarBlue) assay basically tests response to cellular metabolic oxidation – reduction response. Number of live cells determined based on electron density. Colometric (weak fluorescent, blue compound resazurin turn into strong fluorescent, pink compound resozurin) and

spectrophotometric (Thermo Multiskan Go) changes recorded. For imaging H_2O_2 interaction with BOD 2, cells treated with 10 μM H_2O_2, medium washed with PBS, dyed with MitoTracker (ThermoFisher) and after washing, 5 μM BOD 2 administered. After incubation with BOD 2, the cells were washed with PBS buffer and visualized with fluorescent microscope at 20x and 80x. For photocytotoxicity experiment, same procedure used. After incubation of cells, the medium renewed with 10 μM BOD 2 and irradiated with 506 nm LED array for 2 h. Cell viability tested alamarBlue assay.

5.9. Synthesis

All reagents were obtained from commercial suppliers and were used without further purification. All the organic solvents were analytical grade. Column chromatography was performed on silica gel (230–400 mesh, SiliCycle Inc., Canada). Thin-layer chromatography (TLC) was performed on pre-coated silica gel plates (0.25 mm thick, Merck, Germany) and observed under UV light (Handhelp UV Lamp UVGL-58 and Analytik Jena US UVP Chromato-Vue Cabinet C-10). ^{1}H NMR and ^{13}C NMR spectra were recorded at Selçuk University on Varian Inova (400 MHz, d-DMSO or CDCl$_3$) and Varian VXR (400 MHz) spectrometers at room temperature (298 K). HRMS was performed using Agilent 6530 Accurate-Mass Q-TOF LC/MS in Atatürk University.

Reaction was done using modified literature procedure (Xu et al, 2014). Dichloromethane (150 ml) was purged with N$_2$ for 30 minutes. 4-pyridinecarboxyaldehyde (12.7 mmol, 1.36 g, 1.2 ml) was mixed with 2,4 – dimethylpyyrole (26.2 mmol, 2.5 g, 2.6 ml) in degased dichloromethane. Three drops of trifluoroacetic acid (TFA) were added and the color of the solution turned into red. The solution was stirred at room temperature overnight under N$_2$. The reaction was treated with p-chloranil (6.9 mmol, 1.7 g) and the solution was stirred for additional 2.5 hours,
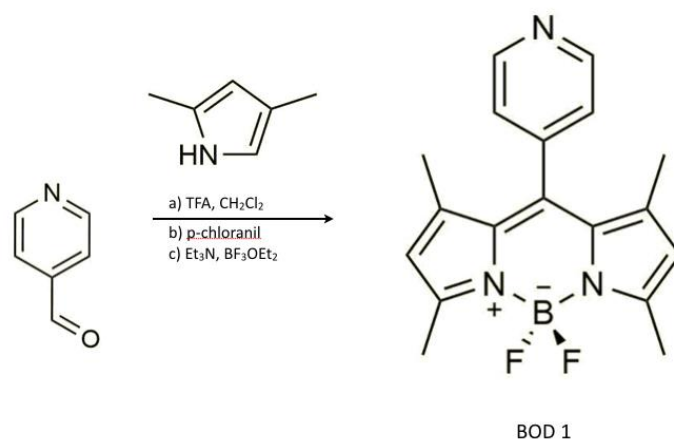
Figure 5.1. Synthesis of compound BOD 1.
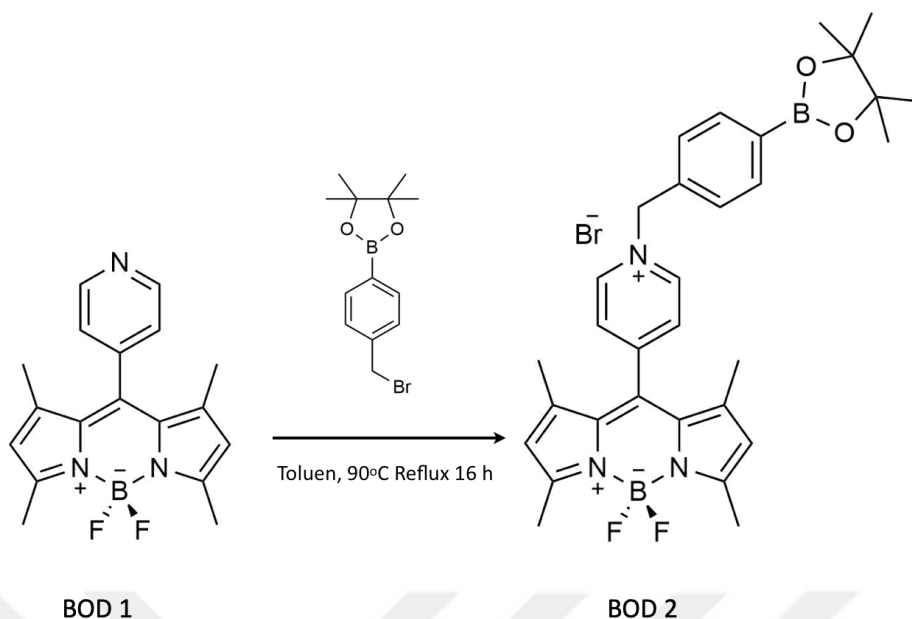
Figure.5.2. Synthesis of compound BOD 2 from BOD 1.

followed by the addition of triethylamine (7.5 ml) and boron trifluoride-diethyl ether complex (7.5 ml). The mixture was stirred for 2.5 hours at room temperature. The crude product was extracted with water and dichloromethane. Organic layer was collected, dried with sodium sulfate and dichloromethane was evaporated in vacuo. The crude product was purified by silica gel column chromotography using %5 methanol in dichloromethane as eluent. The fraction containing BOD1 was collected then the solvent was evaporated under reduced pressure. The product was obtain as glitter red powder (2.5 mmol, 823 mg, 20%).

^{1}H NMR (400 MHz, Chloroform-d) δ 8.78 (d, J = 5.9 Hz, 2H), 7.33 (d, J = 6.0 Hz, 2H), 6.00 (s, 2H), 2.55 (s, 6H), 1.40 (s, 6H). High resolution ESI-MS values are (M+H)+ theoretical : 326.1640 ; experimental:326.1679; Δ: 12 ppm

Reaction was done using modified literature procedure (Xu et al, 2014). 4-(4,4,5,5,-Tetramethyl-1,3,2-dioxaborolan-2-yl)benzyl bromide (0.16 mmol, 47 mg) and BOD1 (0.10 mmol, 34 mg) were dissolved in 10 ml toluen and then solution was refluxed at 90°C for 16 hours. After cooling, the desired product obtained by filtering the precipitate. The red-orange solid was further washed with toluen to afford pure BOD2 (0.05 mmol, 30.8 mg, 49.5%).

^{1}H NMR (400 MHz, DMSO-d$_6$) δ 9.39 (d, J = 5.9 Hz, 1H), 8.47 (d, J = 6.0 Hz, 2H), 7.72 (d, J = 7.5 Hz, 2H), 7.47 (d, J = 7.4 Hz, 2H), 6.26 (s, 2H), 6.00 (s, 2H), 1.35 (s, 6H), 1.33 – 1.19 (m, 12H). High resolution ESI-MS values are M$^+$ theoritical: 542.2962; experimental:542.2961; Δ: 0.18 ppm

APPENDICES

Appendix 1. NMR Spectra
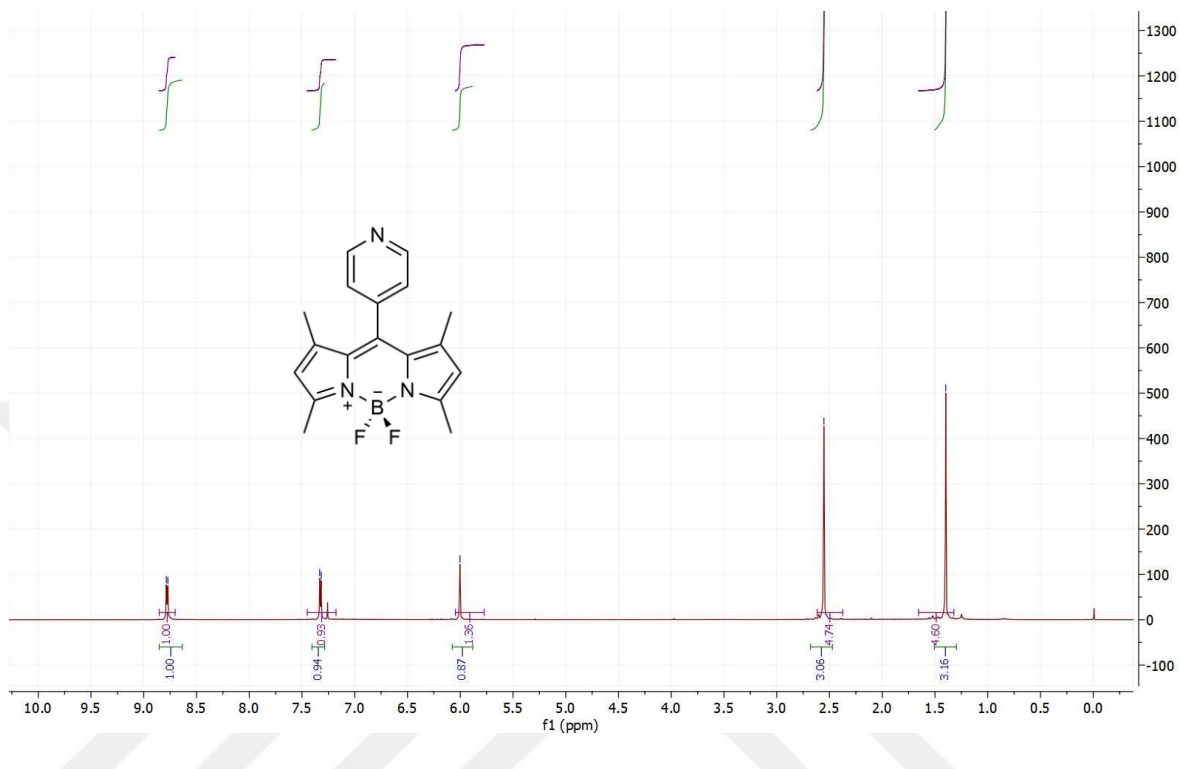
Figure 5.3.^{1}H NMR spectrum of BOD 1 (400 MHz, Chloroform-d).
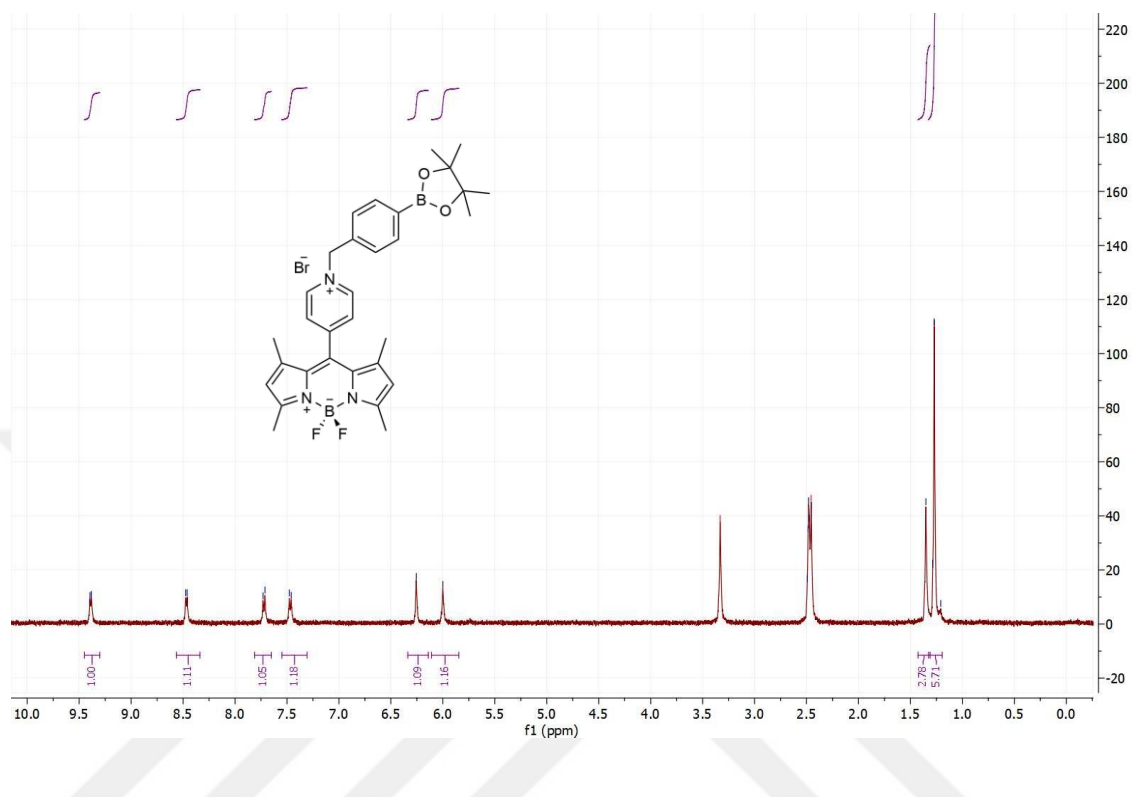
Figure 5.4. ^{1}H NMR spectrum of BOD 2 (400 MHz, DMSO-d$_6$).

Appendix 2. HRMS Spectra

User Spectra

Fragmentor Voltage	Collision Energy	Ionization Mode
60	0	APCI

+APCI Scan (rt: 0.163 min) Frag=60.0V mnzy41.d

x10 5

3.5
3
2.5
2
1.5
1
0.5
0

326.1679
325.1694
327.1700
323.1741
328.1719

321   322   323   324   325   326   327   328   329   330
Counts vs. Mass-to-Charge (m/z)
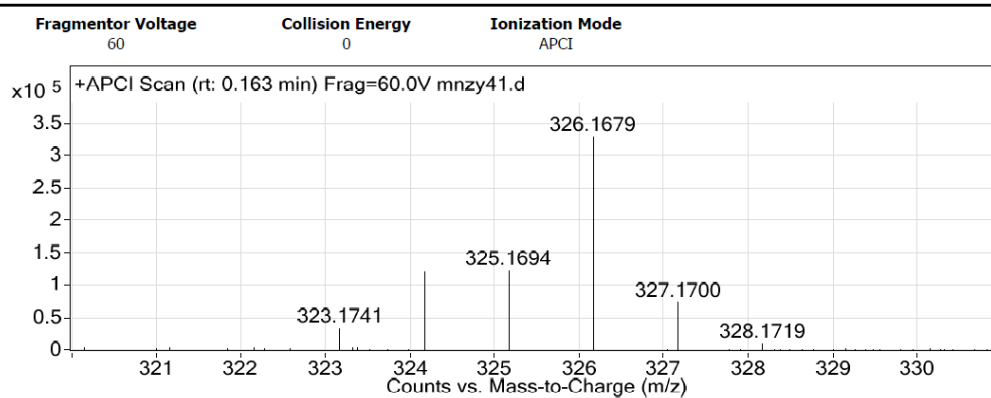
Figure 5.5. High resolution ESI-MS spectrum of BOD 1.

User Spectra

Fragmentor Voltage	Collision Energy	Ionization Mode
60	0	APCI

+APCI Scan (rt: 0 min) Frag=60.0V mnzy-12.d

x10 3

2.5
2
1.5
1
0.5
0

542.2961
543.3069
541.3063

538.5   539   539.5   540   540.5   541   541.5   542   542.5   543   543.5   544   544.5
Counts vs. Mass-to-Charge (m/z)

Figure 5.6. High resolution ESI-MS spectrum of BOD 2.

6. CONCLUSION

In this study a negative feedback control loop is used to regulate the activity of photosensitizer for the first time in literature. A heavy atom free, pyridinium bearing BODIPY molecule (BOD 2) is used as photosensitizer and it has been shown to have efficient photoinduced singlet oxygen production (Figure.5.6). Even though intersystem crossing is reported with similar pyridinium-BODIPYs, for the first time photodynamic action of such halogen-free pyridinium structure is analyzed in this study. Evidences show that designed photosensitizer has no dark toxicity at the micromolar concentrations, have IC$_{50}$ value of 69 μM. Besides, positively charged BOD 2 can pass cell membrane and tends to accumulate in mitochondria where it can show its apoptotic activity better (Figure.5.16). This enables organelle-specific targetting of the photosensitizer. These remarkable properties, such as high photostability, water – solubility, lack of heavy atom, lack of dark toxicity and efficiency at low concentration, show clearly promising new photodynamic agent. Activity of the BOD2 is shown to be reduced through feedback interactions when produced singlet oxygen reacts with sodium ascorbate and generates hydrogen peroxide 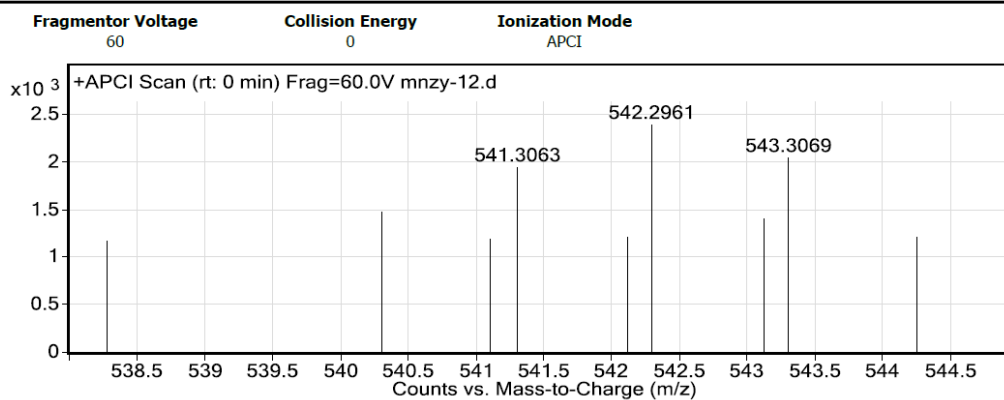(Figure.5.7). Hydrogen peroxide (produced by the reaction of singlet oxygen) converts BOD2 into inactive BOD1 and this maintains a feedback control. Singlet oxygen generation abilities in the presence of various amout of ascorbate supports the proposal (ascorbate generates hydrogen peroxide, which then silence photosensitizer, Figure.4.11). During photodynamic action, absorption spectra shifts from BOD2 spectrum to BOD1 spectrum which further supports the loop reactions taking place during PDT action (Figure.4.15). Effects of BOD2 and BOD1 on cell viability are analyzed and it has been demonstrated that loop conversion product (BOD1) has significantly lower decrease in cell viability (Figure.4.17). It has been demonstrated that upon conversion to BOD1 during photodynamic activity, fluorescence is enhanced in the presence of

ascorbate whereas in the absence of ascorbate lack the ability to create a loop and does not display any enhancement (Figure.4.10). Although there are plenty of activatable photosensitizers in the literature, self-activity control by means of such negative feedback loop is missing. This strategy may provide smarter photodynamic therapy in which agent silences itself once enough damage is given to target tissue. Structure optimization, improvements on the PDT application of optimized structures are planning as future work.

REFERENCES

Albers, A.W., Okreglak, V.S., Chang, C.J., 2006, A FRET-Based Approach to Ratiometric Fluorescence Detection of Hydrogen Peroxide, Journal of the American Chemical Society, 128(30):9640-9641.

Åström, K. J., and Murray, R. M., 2008, Feedback systems: An introduction for scientists and engineers, Princeton: Princeton University.

Awuah, S. G., and You, Y., 2012, Boron dipyrromethene (BODIPY)-based photosensitizers for photodynamic therapy, RSC Advances, 2:11169-11183.

Brilkina, A. A., Peskova, N. N., Dudenkova, V. V., Gorokhova, A. A., Sokolova, E. A., Balalaeva, I. V., 2018, Monitoring of hydrogen peroxide production under photodynamic treatment using protein sensor HyPer, Journal of Photochemistry and Photobiology B: Biology, 178: 296–301.

Cadet, J., and Mascio, P. D., 2009, Peroxides in Biological Systems, PATAIS Chemistry of Functional Groups.

Carloni, P., Damiani, E., Greci, L., Stipa, P., Tanfani, F., Tartaglini, E., Wozniak, M., 1993, On the use of 1,3-diphenylisobenzofuran (DPBF). Reactions with carbon and oxygen centered radicals in model and natural systems, Research on Chemical Intermediates,19(5): 395-405.

Chang, M. C. Y., Pralle, A., Isacoff, E.Y., Chang, C. J., 2004, A Selective, Cell-Permeable Optical Probe for Hydrogen Peroxide in Living Cells. Journal of the American Chemical Society, 126(47):15392-15393.

Chen, B., Pogue, B. W., Hoopes, P. J., Hasan, T., 2005, Combining vascular and cellular targeting regimens enhances the efficacy of photodynamic therapy, International Journal of Radiation Oncology Biology Physics, 61(4):1216-1226.

Chung, C., Srikun, D., Lim, C. S., Chang, C. J., and Cho, B. R., 2011. A two-photon fluorescent probe for ratiometric imaging of hydrogen peroxide in live tissue. Chemical Communications, 47:34, 9618-20.

Cinquin, O., and Demongeot, J., 2002, Roles of positive and negative feedback in biological systems, Comptes Rendus Biologies, 325(11):1085-1095.

Dąbrowski, J. M., Pucelik, B., Regiel-Futyra, A., Brindell, M., Mazuryk, O., Kyzioł, A., and Arnaut, L. G., 2016, Engineering of relevant photodynamic processes through structural modifications of metallotetrapyrrolic photosensitizers, Coordination Chemistry Reviews, 325: 67-101.

Davies, M. J., and Truscott, R. J., 2001, Photo-oxidation of proteins and its role in cataractogenesis, Journal of Photochemistry and Photobiology B: Biology, 63(1-3):114-125.

Dexter, D. L., 1973, Recent Developments in Sensitized Luminescence and Energy Transfer Phenomena in Solids, Luminescence of Crystals, Molecules, and Solutions, 57-63.

Dickinson, B. C., and Chang, C. J., 2008, A Targetable Fluorescent Probe for Imaging Hydrogen Peroxide in the Mitochondria of Living Cells. Journal of the American Chemical Society, 130(30): 9638-9639.

Dougherty, T. J., Gomer, C. J., Henderson, B. W., Jori, G., Kessel, D., Korbelik, M., Moan, J., Peng, Q., 1998, Photodynamic Therapy, Journal of the National Cancer Institute, 90(12), 889-905.

Eckl, D. B., Dengler, L., Nemmert, M., Eichner, A., Bäumler, W., and Huber, H., 2017. A Closer Look at Dark Toxicity of the Photosensitizer TMPyP in Bacteria. Photochemistry and Photobiology,94:1, 165-172.

Forster, T., 1946, Energiewanderung und Fluoreszenz, Die Naturwissenschaften, 33(6): 166-175.

Gollnick, S., 2017, Enhancement of anti-tumor immunity by PDT: Mechanisms and exploitation, Photodiagnosis and Photodynamic Therapy,17.

Gomer, C. J., and Razum, N. J., 1984, Acute Skin Response In Albino Mice Following Porphyrin Photosensitization Under Oxic And Anoxic Conditions, Photochemistry and Photobiology, 40(4):435-439.

Harriman, A., Mallon, L. J., Ulrich, G., Ziessel, R., 2007, Rapid Intersystem Crossing in Closely-Spaced but Orthogonal Molecular Dyads, ChemPhysChem, 8(8):1207-1214.

Hellman, B., 2009, Pulsatility of insulin release – a clinically important phenomenon,

Upsala Journal of Medical Sciences, 114(4): 193-205.

Holling, C. S., 1973, Resilience and Stability of Ecological Systems, Annual Review of Ecology and Systematics, 4(1): 1-23.

Jacob, F., Monod, J., 1989, Genetic Regulatory Mechanisms in the Synthesis of Proteins, Molecular Biology, 82-120.

Jang, W., Nakagishi, Y., Nishiyama, N., Kawauchi, S., Morimoto, Y., Kikuchi, M., and Kataoka, K., 2006, Polyion complex micelles for photodynamic therapy: Incorporation of dendritic photosensitizer excitable at long wavelength relevant to improved tissue-penetrating property, Journal of Controlled Release,113(1): 73-79.

Josefsen L.B. and Boyle R.W., 2008, Photodynamic Therapy and the Development of Metal – based Photosensitizers, Met Based Drugs, 2008: 276109.

Kamkaew, A., Lim, S. H., Lee, H. B., Kiew, L. V., Chung, L. Y., Burgess, K., 2013, BODIPY dyes in photodynamic therapy, Chem. Soc. Rev., 42(1): 77-88.

Kessel D. and Oleinick N.L., 2009. Initiation of autophagy in photodyanmic therapy. Methods Enzymol 453:1—16.

Korneev, K. V., Atretkhany, K. N., Drutskaya, M. S., Grivennikov, S. I., Kuprash, D. V., Nedospasov, S. A., 2017, TLR-signaling and proinflammatory cytokines as drivers of tumorigenesis, Cytokine, 89: 127-135.

Kramarenko, G. G., Hummel, S. G., Martin, S. M., Buettner, G. R., 2006, Ascorbate Reacts with Singlet Oxygen to Produce Hydrogen Peroxide, Photochemistry and

Photobiology, 82(6): 1634-1637.

Lakowicz, J. R., 2010**.** Principles of fluorescence spectroscopy. New York: Springer**.**

Lampard, E. V., Sedgwick, A. C., Sun, X., Filer, K. L., Hewins, S. C., Kim, G., Yoon, J., Bull, S. D., James, T. D., 2018, Boronate-Based Fluorescence Probes for the Detection of Hydrogen Peroxide. Chemistry Open Communications, 7:262 – 265.

Lau, A. Y., and Roux, B., 2011, The Hidden Energetics of Ligand-Binding and Activation in a Glutamate Receptor, Nature Structural and Molecular Biology, 18(3): 283-7.

Lippert, A. R., Van de Bittner, G. C., Chang, C. J., 2011, Boronate oxidation as a bioorthogonal reaction approach for studying the chemistry of hydrogen peroxide in living systems, Accounts of chemical research, 44(9):793 – 804.

Loudet, A., and Burgess, K., 2007, BODIPY dyes and their derivatives: syntheses and spectroscopic properties, Chemical reviews, 107(11): 4891-4932.

Lovell, J. F., Chan, M. W., Qi, Q., Chen, J., Zheng, G., 2011, Porphyrin FRET Acceptors for Apoptosis Induction and Monitoring, Journal of the American Chemical Society, 133(46):18580-18582.

Lovell, J. F., Liu, T. W., Chen, J., Zheng, G., 2010, Activatable Photosensitizers for Imaging and Therapy, Chemical Reviews,110(5): 2839-2857.

Marian, C. M., 2011, Spin-orbit coupling and intersystem crossing in molecules, Wiley

Interdisciplinary Reviews: Computational Molecular Science, 2(2):187-203.

Mclaughlin, B., Surender, E. M., Wright, G. D., Daly, B., and Silva, A. P., 2018, Lighting-up protein–ligand interactions with fluorescent PET (photoinduced electron transfer) sensor designs, Chemical Communications, 54(11): 1319-1322.

Miller, E. W., Albers, A. E., Pralle, A., Isacoff, E. Y., Chang, C. J., 2005, Boronate-Based Fluorescent Probes for Imaging Cellular Hydrogen Peroxide, Journal of the American Chemical Society, 127(47):16652-16659.

Miller, E. W., Tulyathan, O., Isacoff, E. Y., Chang, C. J., 2007, Molecular Imaging of Hydrogen Peroxide Produced for Cell Singaling, Nature Chemical Biology, 3(5): 263 – 267.

Murphy, M. P., 2008, Targeting Antioxidants to Mitochondria by Conjugation to Lipophilic Cations, Drug-Induced Mitochondrial Dysfunction, 575-587.

Nestler, E. J., 2015, Molecular neuropharmacology: A foundation for clinical neuroscience. New York: McGraw-Hill.

Portera C.A., Berman R.S., and Ellis L.M., 1998. Molecular determinants of colon cancer metastasis. Surg Oncol 7:183—95.

Prime, J., 1900, Accidents Toxiques Prodult par l'Eosinate se Sodium, 2nd edition Paris:Jouve et Boyer.

Pshenichnyuk, S. A., Modelli, A., Lazneva, E. F., Komolov, A. S., 2016, Hypothesis

for the Mechanism of Ascorbic Acid Activity in Living Cells Related to Its Electron-Accepting Properties. The Journal of Physical Chemistry A,120(17):2667-2676).

Raab O., 1900, Uber die Wirkung fluoreszierender Stoffe auf Infusorien, Z Biol, 39:524-546.

Robertson, C., Evans, D. H., Abrahamse, H., 2009, Photodynamic therapy (PDT): A short review on cellular mechanisms and cancer research applications for PDT, Journal of Photochemistry and Photobiology B: Biology,96(1): 1-8.

Schmitz, C., Aubry, J. M., Rigaudy, J.,1982, ChemInform Abstract: A New Access To The Anthracene Core. Synthesis Of Two Water-Soluble Singlet Oxygen Traps Derived From 1,3-Diphenylisobenzofuran And 9,10-Diphenylanthracene, Chemischer Informationsdienst, 13(40).

Sharman, W. M., Allen, C. M., Lier, J. E., 1999, Photodynamic therapeutics: Basic principles and clinical applications, Drug Discovery Today, 4(11): 507-517.

Silva, A. P., Gunaratne, H. Q., Gunnlaugsson, T., Huxley, A. J., Mccoy, C. P., Rademacher, J. T., Rice, T. E., 1997, Signaling Recognition Events with Fluorescent Sensors and Switches, Chemical Reviews, 97(5): 1515-1566.

Skovsen, E., Snyder, J.W., Lambert, J.D.C, Ogilby, P.R., 2005, Lifetime and Diffusion of Singlet Oxygen in a Cell, The Journal of Physical Chemistry B., 109(18): 8570-8573.

Stokes, G. G., 1852, On the Change of Refrangibility of Light. Mathematical and Physical Papers, 267-414.

Tian, J., Zhou, J., Shen, Z., Ding, L., Yu, J., Ju, H., 2015, A pH-activatable and aniline-substituted photosensitizer for near-infrared cancer theranostics, Chemical Science, 6(10): 5969-5977.

Valeur, B., and Berberan-Santos, M. N., 2012, Molecular fluorescence: Principles and applications, John Wiley and Sons.

Vlahopoulos, S. A., Cen, O., Hengen, N., Agan, J., Moschovi, M., Critselis, E., Chrousos, G. P., 2015, Dynamic aberrant NF-κB spurs tumorigenesis: A new model encompassing the microenvironment, Cytokine and Growth Factor Reviews, 26(4): 389-403.

Von Tappeiner H. and Jesionek A., 1903, Therapeutische Versuche mit fluoreszierenden Stoffen, Muench Med Wochenschr, 47:2042-2044.

Von Tappeiner H. and Jodlbauer A., 1904, Uber die Wirkung der photodynamischen (fluoreszierenden) Stoffen auf Infusorien, Etsch Arch Klin Med., 80:427-487

Wang, D., Miyamoto, R., Shiraishi, Y., Hirai, T., 2009, BODIPY-Conjugated Thermoresponsive Copolymer as a Fluorescent Thermometer Based on Polymer Microviscosity, Langmuir, 25(22):13176-13182.

Wang, X., Wang, H., Zhang, L., Guo, M., Huang, Z., 2010, Topical ALA PDT for the treatment of severe acne vulgaris, Photodiagnosis and Photodynamic Therapy,7(1): 33-38.

Warburg O., Posener K., Negelein E., 1924. Über den Stoffwechsel der Tumoren (On metabolism of tumors) Biochem Z.,152:319–344.

Wen J, Matsumoto K, Taniura N, Tomioka D, Nakamura T., 2007. Inhibition of colon cancer growth and metastasis by NK4 gene repetitive delivery in mice. Biochem Biophys Res Commun 358:17—23.

Wotherspoon, T., and Hübler, A., 2009, Adaptation to the Edge of Chaos with Random-Wavelet Feedback, The Journal of Physical Chemistry A, 113(1):19-22.

Wright, A., 2003, Photo-oxidation of cells generates long-lived intracellular protein peroxides. Free Radical Biology and Medicine, 34(6): 637-647.

Xu, J., Li, Q., Yue, Y., Guo, Y., Shao, S., 2014, A water-soluble BODIPY derivative as a highly selective "Turn-On" fluorescent sensor for H2O2 sensing in vivo, Biosensor and Bioelectronics, 56: 58 – 63.

Zhang, J., Ji, X., Zhou, J., Chen, Z., Dong, X., Zhao, W., 2018, Pyridinium substituted BODIPY as NIR fluorescent probe for simultaneous sensing of hydrogen sulphide/glutathione and cysteine/homocysteine, Sensors and Actuators B: Chemical, 257: 1076-1082

Zhang, J., Jiang, C., Longo, J. P., Azevedo, R. B., Zhang, H., and Muehlmann, L. A., 2018, An updated overview on the development of new photosensitizers for anticancer photodynamic therapy, Acta Pharmaceutica Sinica B, 8(2): 137-146.

Zhao, J., Huang, L., Cui, X., Li, S., and Wu, H., 2015, Maximizing the thiol-activated photodynamic and fluorescence imaging functionalities of theranostic reagents by modularization of Bodipy-based dyad triplet photosensitizers, Journal of Materials Chemistry B, 3(47): 9194-9211.

Zhao, Q., Yin, C., Kang, J., Wen, Y., Huo, F., 2018, A viscosity sensitive azide-pyridine BODIPY-based fluorescent dye for imaging of hydrogen sulfide in living cells, Dyes and Pigments, 159: 166-172.